LUND UNIVERSITY

Superfluidity and Supersolidity in Ultracold Atomic Gases Beyond Mean Field

Nilsson Tengstrand, Mikael

2022

Superfluidity and Supersolidity in Ultracold Atomic Gases Beyond Mean Field

MIKAEL NILSSON TENGSTRAND
DEPARTMENT OF PHYSICS | FACULTY OF ENGINEERING | LUND UNIVERSITY
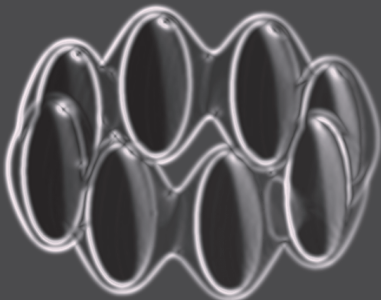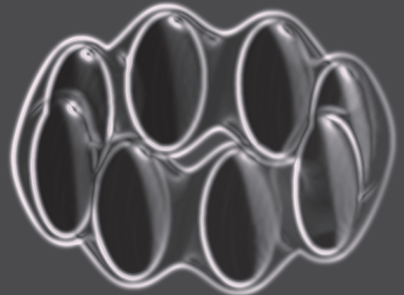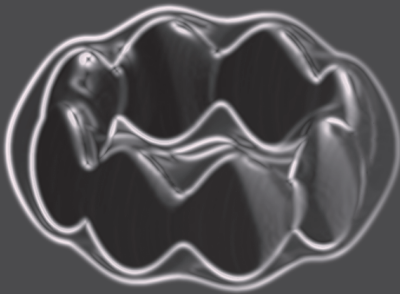
Superfluidity and Supersolidity in Ultracold Atomic Gases
Beyond Mean Field

Superfluidity and Supersolidity in Ultracold Atomic Gases Beyond Mean Field

by Mikael Nilsson Tengstrand

LUND

UNIVERSITY

Thesis for the degree of Doctor of Philosophy in Engineering
Thesis advisor: Stephanie M. Reimann
Faculty opponent: Alessio Recati

Abstract

This thesis investigates ultracold bosonic systems using an extended mean-field formalism with a focus on their superfluid and supersolid properties. The dissertation comprises five chapters and four articles, where the chapters provide some background to the research put forward in articles.

Paper I demonstrates the existence of multiple singly-quantized vortices in two-dimensional droplets made out of binary Bose mixtures, and discusses the possibility of using metastable persistent currents to generate self-bound vortex-carrying states.

Paper II studies metastable persistent flow in dipolar supersolids in ring-shaped trapping potentials and gives a criterion for when such flow can exist. Hysteretic effects are investigated and found to depend qualitatively on the fraction of non-classical rotational inertia of the system.

Paper III presents results regarding the validity of using a super-Gaussian ansatz when describing two-dimensional self-bound droplets in Bose-Bose mixtures, and it is found that most quantities are well-described by employing such an ansatz. Furthermore, the breathing mode of droplets with and without vorticity is studied.

Paper IV investigates droplet-superfluid compounds in one-dimensional binary Bose mixtures trapped by means of periodic boundary conditions. It is found that such configurations have a fraction of non-classical rotational inertia larger than zero but smaller than unity at zero temperature. It is demonstrated that this fraction is not equal to the residual superfluid part of the system due to the superfluid's response to the motion of the localized parts.

DOKUMENTDATABLAD enl SIS 61 41 21

Signature _____   Date _____2022-03-14_____

Superfluidity and Supersolidity in Ultracold Atomic Gases Beyond Mean Field

by Mikael Nilsson Tengstrand

LUND
UNIVERSITY

A doctoral thesis at a university in Sweden takes either the form of a single, cohesive research study (monograph) or a summary of research papers (compilation thesis), which the doctoral student has written alone or together with one or several other author(s).

In the latter case the thesis consists of two parts. An introductory text puts the research work into context and summarizes the main points of the papers. Then, the research publications themselves are reproduced, together with a description of the individual contributions of the authors. The research papers may either have been already published or are manuscripts at various stages (in press, submitted, or in draft).

Cover illustration front: Density isosurfaces of a dipolar condensate in a toroidal trap.

Faculty of Engineering, LTH, Department of Physics
Division of Mathematical Physics

Contents

Acknowledgements

List of publications and contributions of the author

This thesis is based on the following publications, referred to by their Roman numerals:

I   **Rotating Binary Bose-Einstein Condensates and Vortex Clusters in Quantum Droplets**

   M. Nilsson Tengstrand, P. Stürmer, E. Ö. Karabulut, and S. M. Reimann
   Phys. Rev. Lett. **123**, 160405 (2019)

   Contributions: I contributed to the conceptualization of the project, wrote the code, did some of the simulations, and wrote the first draft.

II   **Persistent currents in toroidal dipolar supersolids**

   M. Nilsson Tengstrand, D. Boholm, R. Sachdeva, J. Bengtsson, and S. M. Reimann
   Phys. Rev. A **103**, 013313 (2021)

   Contributions: I contributed to the conceptualization of the project, wrote the code, did some of the simulations, made the model of the system, did the analytical calculations, and wrote the first draft.

III   **Breathing mode in two-dimensional binary self-bound Bose-gas droplets**

   P. Stürmer, **M. Nilsson Tengstrand**, R. Sachdeva, and S. M. Reimann
   Phys. Rev. A **103**, 053302 (2021)

   Contributions: I wrote a core part of the code, did some of the analytical calculations, and participated in the analysis.

IV   Droplet-superfluid compounds in binary bosonic mixtures

M. Nilsson Tengstrand and S. M. Reimann

Contributions: I contributed to the conceptualization of the project, wrote the code, did some of the simulations, made the model of the system, did the analytical calculations, and wrote the first draft.

Publications not included in this thesis:

Quantum Szilard Engine with Attractively Interacting Bosons

J. Bengtsson, **M. Nilsson Tengstrand**, A. Wacker, P. Samuelsson, M. Ueda, H. Linke, and S. M. Reimann

Bosonic Szilard engine assisted by Feshbach resonances

J. Bengtsson, **M. Nilsson Tengstrand**, and S. M. Reimann

Self-bound supersolid stripe phase in binary Bose-Einstein condensates

R. Sachdeva, **M. Nilsson Tengstrand**, S. M. Reimann

Popular Science Summary

How simple is too simple? When scientists attempt to model reality it often leads to making assumptions and approximations. If we for example wish to predict how many will be infected by a virus we could simplify our model by neglecting reinfections, by approximating the population distribution to be homogeneous, by assuming that individuals interact randomly and so forth. How well a model describes the real world depends crucially on these assumptions: if they are good they should lead to nothing more than small quantitative deviations; if they are not the results could be qualitatively different. In the world of cold atomic gases where this thesis takes place it is often possible to obtain an accurate theoretical description by means of so-called mean-field theory. Mean-field theory, while incorporating many approximations, can in many cases be motivated on the basis of an excellent agreement with experiments. This is not always the case however, and there are situations where mean-field theory fails to capture the essential physics. In these instances one has to go beyond the mean-field description, and it was recently realized that a whole world of exciting physics awaits there to be investigated.

The systems investigated theoretically in this thesis are cold. In fact, the temperatures achieved in the corresponding experiments can be very close to zero kelvin, or -273.15 degrees Celsius. When a collection of atoms of a type known as bosons are cooled down to these low temperatures they can change phase into a Bose-Einstein condensate, a curious state of matter that exhibits quantum behavior even on a macroscopic scale. These condensates have strong ties to two other types of physical phenomena relevant to this thesis, namely superfluidity and supersolidity. Superfluids have zero viscosity (a measure of a fluid's thickness) and can flow without losing energy. When put in a rotating container, these thin fluids can form vortices that continue to rotate for a long time even after the container is brought to rest, thus holding a current that flows persistently. Supersolidity is the conceptual marriage between superfluidity and solidity, and combines the notion of a rigid structure with that of frictionless flow, an idea that quickly conspires to wage war with our intuition!

In this thesis we study superfluidity and supersolidity in the context of ultracold gases where mean-field theory breaks down, aiming to contribute to the general body of knowledge for these concepts in the spirit of basic research. In particular, we find in Paper 1 that lattices of vortices may exist in two-dimensional self-bound

droplets, and suggest how vortical droplets could be created experimentally. In Paper II we investigate the rotational properties of a three-dimensional dipolar supersolid trapped in a ring and identify the conditions for the existence of meta-stable persistent currents. Paper III examines the validity of using a particular mathematical method to describe two-dimensional droplet systems, finding that this method in many cases provides an excellent description. Finally, in Paper IV we study the interplay of superfluidity and localization in a one-dimensional ring, and shed some light on the consequences of the connection between localized and non-localized components.

Populärvetenskaplig Sammanfattning

Hur enkel får en vetenskaplig beskrivning lov att vara? När forskare modellerar världen behöver de ofta göra många antaganden och approximationer. Om vi till exempel vill förutspå hur många som kommer att bli infekterade av ett virus så kan vi simplifiera vår modell genom att inte ta hänsyn till återinfektioner, anta att folk interagerar helt slumpmässigt, approximera befolkningstätheten som konstant och så vidare. Hur dessa simplifieringar väljs är helt avgörande för hur bra modellen kommer att beskriva verkligheten: om de är väl valda så borde de inte leda till mer än små kvantitativa fel; om de inte är det så kan resultaten bli kvalitativt olika jämfört vad som faktiskt händer. I det forskningsfält som studerar iskalla atomgaser där denna avhandling tar plats så är det ofta möjligt att få en bra teoretisk beskrivning med så kallad medelfältsteori. Trots att medelfältsteori använder sig av många approximationer så kan denna i många fall motiveras genom god överenstämmelse med experiment. Detta är dock inte alltid fallet, och det finns situationer där medelfältsteori misslyckas helt att beskriva fysiken korrekt. I dessa fall måste man gå bortom medelfältsbeskrivningen, och det insågs nyligen att det finns massvis av spännande fysik som inte har kartlagts där.

De system som studerats teoretiskt i denna avhandling är kalla, så kalla att de temperaturer som uppnås i motsvarande experiment är mycket nära noll kelvin, eller -273.15 grader Celsius. När en samling partiklar av en typ som kallas bosoner kyls ner till dessa låga temperaturer så kan de bli ett Bose-Einstein kondensat, ett märkligt aggregationstillstånd som uppvisar kvantmekaniska effekter även på en makroskopisk nivå. Dessa kondensat har starka anknytningar till två fysikaliska fenomen som är relevanta för denna avhandling, nämligen suprafluiditet och suprasoliditet. Suprafluider har noll viskositet (vilket är ett mått på en vätskas tjocklek) och kan flöda utan att förlora energi. När denna typ av fluid placeras i en roterande bägare kan det bildas virvlar som fortsätter snurra en lång tid efter att bägaren slutat rotera, det vill säga det finns alltså kvar ett bestående flöde. Suprasoliden är en typ av materia som har både en stel strukur associerad med det fasta tillståndet samt suprafluidens flödesegenskaper, en idé som kan kännas ytterst paradoxal!

I denna avhandling undersöker vi suprafluiditet och suprasoliditet hos kalla atomgaser i den regim där medelfältsteori inte är en bra beskrivning av verkligheten, med målet att utöka förståelsen för dessa fascinerande koncept i grundforskningens anda. Mer specifikt så finner vi i Artikel 1 att ett gitter av virvlar kan existera i tvådimensionella självbundna droppar, och föreslår hur kvantdroppar med virvlar

skulle kunna skapas experimentellt. I Artikel II undersöker vi rotationsegenskaperna hos en tredimensionell suprasolid i en badringsformad bägare och identifierar vad som ska krävas för att det ska existera bestående flöden. Artikel III undersöker hur väl en speciell matematisk metod beskriver tvådimensionella system av självbundna droppar, och det visar sig att denna metod fungerar mycket väl. Slutligen i Artikel IV studerar vi kopplingen mellan suprafluiditet och lokalisering i ett endimensionellt system, och visar på några konsekvenser av samspelet mellan lokaliserade och icke lokaliserade delar.

Part I

Background and Theory

Chapter 1

Introduction

The states of matter most commonly encountered throughout everyday life number three: solids, characterized by the ability to retain their shape and volume against external forces; liquids, which change shape according to the surroundings at an approximately constant volume; and gases, which will adapt both shape and volume according to an external confinement. These are not the only ways in which nature may present itself to us, and it turns out that there is an abundance of matter configurations that do not fit into the three aforementioned categories. One of these and the main topic of this thesis is Bose-Einstein condensation, where at least one quantum state becomes macroscopically populated. Theorized in 1924 [1, 2], a transition to this state of matter can occur when a collection of bosons are cooled down to temperatures close to absolute zero. Following the first experimental realizations in cold atomic gases in 1995 [3–5], these systems have provided an excellent space to conduct basic research, both experimentally due to a high degree of control and tunability, and theoretically due to the dilute and weakly-interacting nature of these atomic systems which often allows for simple and accurate descriptions. Although curious on their own, Bose-Einstein condensates may exhibit further exotic behavior, such as superfluidity and supersolidity. First observed in helium [6, 7], a superfluid can flow without friction at zero viscosity. A supersolid on the other hand has both superfluid and solid properties at the same time [8–12], a notion that may seem counterintuitive. Despite their strange nature, evidence for the existence of these supersolids has been found experimentally with several kinds of bosonic quantum gases [13–17].

In the context of dilute atomic gases, Bose-Einstein condensates can often be successfully modelled by using mean-field methods. While it is possible to include perturbative corrections to these mean-field descriptions [18–22], this often does not affect the physics in a significant manner since the mean-field contribution usually dominates for dilute and weakly-interacting gases. A different scenario may arise in Bose-Bose mixtures with short-range interactions, where it was predicted for a three-dimensional system in certain parameter regimes that attractive mean-field and repulsive beyond mean-field contributions to the energy may compete in a way that results in self-bound droplet states [23], thus predicting qualitatively different physics compared to the mean-field picture where a collapse of the condensate is expected for the same parameters [24, 25]. Following this theoretical prediction droplets of a conceptually similar kind were observed in the laboratory [26–29], although in a different type of configuration with only a single component consisting of strongly dipolar atoms. Shortly thereafter it was shown that these dipolar droplets could be described theoretically by including beyond mean-field corrections [30–34], in analogy with the situation for binary mixtures. The droplets corresponding to the original prediction in binary systems were eventually also found experimentally [35, 36], but this would not be the end of this story. In the same beyond mean-field formalism as for the droplets, it was suggested that trapped dipolar condensates could display supersolid behavior [37, 38], which was also found experimentally [15–17]. Another example of physics not captured by mean-field theory has been proposed for repulsive Bose-Bose mixtures, where higher-order corrections can break the miscibility-immiscibility dichotomy and lead to a new mixed-bubble phase, where a mixed phase coexists with a pure phase of one of the components [39]. Given the abovementioned examples, one can only speculate what new types of physics await to be uncovered, and it remains to be seen what the future holds for the field of ultracold atomic physics.

This thesis is centered around the topics introduced in the above two paragraphs, investigating superfluid and supersolid properties of Bose-Einstein condensates beyond mean field. The following chapters do not aim to be a complete review the field, but rather attempt to provide some relevant background to the articles of this thesis. Chapter 2 focuses on the beyond mean-field formalism for Bose systems, chapter 3 and 4 discuss the concepts of superfluidity and supersolidity, respectively, and chapter 5 concludes the thesis. Finally, the papers that constitute the novel research of this dissertation are presented in their entirety at the end.

Chapter 2

Mean-Field Theory and Beyond

It all has to start somewhere, and that somewhere is in our case a non-linear differential equation. Where does this equation come from? The short answer is the Schrödinger equation; a longer answer, amalgamating the author's understanding with the literature, can be found in this chapter.

Note that in this and the following chapters we will always work in dimensionless units such that $\hbar = k_B = m = 1$, where $\hbar$ is Planck's reduced constant, k_B the Boltzmann constant, and m the mass of a single particle (in the case where there are two different types of particles we set $m_1 = m_2 = 1$).

2.1   Bose-Einstein Condensation

The Penrose-Onsager definition[1] of a Bose-Einstein condensate starts by considering the eigenvalue equation [40]

$$\int d\mathbf{r}' n^{(1)}(\mathbf{r}, \mathbf{r}', t)\psi_i(\mathbf{r}', t) = \gamma_i(t)\psi_i(\mathbf{r}, t), \qquad (2.1)$$

where $n^{(1)}(\mathbf{r}, \mathbf{r}', t) = \langle \hat{\Psi}^\dagger(\mathbf{r}, t)\hat{\Psi}(\mathbf{r}', t) \rangle$ is the one-body density matrix and $\hat{\Psi}$ the

---

[1]There are several ways to define Bose-Einstein condensation; this definition is particularly useful since it applies to a large class of systems.

bosonic field operator. The orthonormal functions ψ_i constitute a natural basis that diagonalizes $n^{(1)}$, which may be written

$$n^{(1)}(\mathbf{r}, \mathbf{r}', t) = \sum_i \gamma_i(t)\psi_i^*(\mathbf{r}, t)\psi_i(\mathbf{r}', t). \tag{2.2}$$

Bose-Einstein condensation is defined to occur when at least one of the eigenvalues γ_i is of the same order as the total particle number N. When precisely one of these eigenvalues is of order N the condensate is called simple, otherwise fragmented [41]. We now consider a simple condensate and write

$$n^{(1)}(\mathbf{r}, \mathbf{r}', t) = \gamma_0(t)\psi_0^*(\mathbf{r}, t)\psi_0(\mathbf{r}', t) + \sum_{i \neq 0} \gamma_i(t)\psi_i^*(\mathbf{r}, t)\psi_i(\mathbf{r}', t), \tag{2.3}$$

where the zero index corresponds to the largest eigenvalue i.e. the condensed state. In the case where $|\mathbf{r}' - \mathbf{r}|$ is large one might expect the terms with $i \neq 0$ to interfere destructively such that the second term in Eq. (2.3) goes to zero and $n^{(1)} \to \gamma_0\psi_0^*\psi_0 \neq 0$. This property is referred to as off-diagonal long-range order, and its existence is sometimes taken as the definition for Bose-Einstein condensation. To be a bit more explicit, consider the example of a time-independent non-interacting uniform system in a volume V. The eigenfunctions are then plane waves $\psi_{\mathbf{k}}(\mathbf{r}) = e^{i\mathbf{k}\cdot\mathbf{r}}/\sqrt{V}$ with eigenvalues

$$\gamma_{\mathbf{k}} = \frac{1}{e^{\beta(\epsilon_{\mathbf{k}}-\mu)} - 1}, \tag{2.4}$$

where $\mu < 0$ is the chemical potential, $\beta = 1/T$ the inverse temperature, and $\epsilon_{\mathbf{k}} = k^2/2$. By approximating $\gamma_{\mathbf{k}} \approx T/(\epsilon_{\mathbf{k}} - \mu)$ and taking the sum to an integral the second term in Eq. (2.3) becomes

$$T \int \frac{d\mathbf{k}}{(2\pi)^3} \frac{e^{i\mathbf{k}\cdot(\mathbf{r}'-\mathbf{r})}}{k^2/2 - \mu}, \tag{2.5}$$

which can be evaluated to [42]

$$n^{(1)}(\mathbf{r}, \mathbf{r}') = \frac{\gamma_0}{V} + T \frac{e^{-\sqrt{-2\mu}|\mathbf{r}'-\mathbf{r}|}}{2\pi|\mathbf{r}' - \mathbf{r}|}, \tag{2.6}$$

showing that the second term goes to zero for $|\mathbf{r}' - \mathbf{r}| \to \infty$ while $n^{(1)}$ is non-vanishing in the same limit. It should be noted that off-diagonal long-range order as a definition for Bose-Einstein condensation becomes problematic when one for example considers a trapped condensate, where the limit $|\mathbf{r}' - \mathbf{r}| \to \infty$ can not be applied in a meaningful way.

The order of magnitude differences between the eigenvalues and the form of the one-body density matrix in Eq. (2.3) motivates a similar separation for the field operator:

$$\hat{\Psi}(\mathbf{r}, t) = \Phi(\mathbf{r}, t) + \hat{\eta}(\mathbf{r}, t), \tag{2.7}$$

where $\Phi = \langle \hat{\Psi} \rangle$ is a classical field describing the condensed state and $\hat{\eta}$ a fluctuation operator accounting for the rest of the states [24, 43, 44]. Some discussion is warranted regarding the expectation value $\Phi = \langle \hat{\Psi} \rangle$, which at $T = 0$ is taken with respect to an eigenstate of some Hamiltonian. This expectation value can not be non-zero if the Hamiltonian commutes with the number operator, i.e. for a definite particle number. A way out of this is to work with Bogoliubov quasi-averages [45], where one adds to the Hamiltonian the small term

$$\lim_{\lambda \to 0^+} \lambda \int d\mathbf{r} \left[\hat{\Psi}(\mathbf{r}, t)e^{-i\theta} + \hat{\Psi}^\dagger(\mathbf{r}, t)e^{i\theta} \right], \tag{2.8}$$

where λ and θ are real numbers. The reasoning for this idea can be motivated for example in the case of a Heisenberg ferromagnet, where the Hamiltonian possesses a rotational $O(3)$ symmetry [45]. Below the Curie temperature a fraction of the system's spins all point in the same direction, however because of the symmetry the expectation value of the magnetization vector is necessarily zero. The addition of a small external magnetic field breaks this symmetry and causes the spins to point along this field such that the expectation value of the magnetization vector can be non-zero. In the same line of thought the term in Eq. (2.8) takes the role of the external magnetic field and breaks the commutation of the Hamiltonian with the number operator, allowing for $\langle \hat{\Psi} \rangle$ to be different from zero. The addition

of this term corresponds to breaking the global $U(1)$ symmetry inherent to the original Hamiltonian, and the quantity Φ is referred to as the order parameter since it is non-zero only in the condensed phase where global gauge symmetry is spontaneously broken [44].

2.2 One-Component Bose Systems

We consider first N identical bosons at zero temperature described by the Hamiltonian

$$
\begin{aligned}
\hat{H} = &\int d\mathbf{r}\, \hat{\Psi}^\dagger(\mathbf{r}, t) h_0(\mathbf{r}, t)\hat{\Psi}(\mathbf{r}, t) \\
&+ \frac{1}{2}\iint d\mathbf{r}'d\mathbf{r}\, \hat{\Psi}^\dagger(\mathbf{r}', t)\hat{\Psi}^\dagger(\mathbf{r}, t) V_{\text{int}}(\mathbf{r}' - \mathbf{r})\hat{\Psi}(\mathbf{r}', t)\hat{\Psi}(\mathbf{r}, t),
\end{aligned}
\tag{2.9}
$$

where $V_{\text{int}}(\mathbf{r})$ is the two-body interaction potential and $h_0(\mathbf{r}, t) = -\nabla^2/2 + V_{\text{ext}}(\mathbf{r}, t)$ with the external potential $V_{\text{ext}}(\mathbf{r}, t)$. The central approximation in our description of the condensate is the separation of the field operator into two parts according to Eq. (2.7). This approximation results in a Hamiltonian that does not commute with the number operator $\hat{N} = \int d\mathbf{r}\, \hat{\Psi}^\dagger(\mathbf{r}, t)\hat{\Psi}(\mathbf{r}, t)$, and it is convenient to work with the grand-canonical Hamiltonian $\hat{K} = \hat{H} - \mu\hat{N}$ [46, 47], where μ is the chemical potential and $N = \langle\hat{N}\rangle$ is the total average number of particles. The Heisenberg equation of motion for the field operator with respect to the grand-canonical Hamiltonian is

$$
i\frac{\partial\hat{\Psi}(\mathbf{r}, t)}{\partial t} = h(\mathbf{r}, t)\hat{\Psi}(\mathbf{r}, t) + \int d\mathbf{r}'\, \hat{\Psi}^\dagger(\mathbf{r}', t) V_{\text{int}}(\mathbf{r}' - \mathbf{r})\hat{\Psi}(\mathbf{r}', t)\hat{\Psi}(\mathbf{r}, t), \tag{2.10}
$$

where $h(\mathbf{r}, t) \equiv h_0(\mathbf{r}, t) - \mu(t)$. An equation of motion for the order parameter can be obtained by taking the expectation value of both sides of Eq. (2.10) and using Eq. (2.7), resulting in

$$i\frac{\partial \Phi(\mathbf{r},t)}{\partial t} = h(\mathbf{r},t)\Phi(\mathbf{r},t) + \int d\mathbf{r}' V_{\text{int}}(\mathbf{r}'-\mathbf{r})|\Phi(\mathbf{r}',t)|^2\Phi(\mathbf{r},t)$$

$$+ \int d\mathbf{r}' V_{\text{int}}(\mathbf{r}'-\mathbf{r})\Big[\Phi^*(\mathbf{r}',t)\langle\hat{\eta}(\mathbf{r}',t)\hat{\eta}(\mathbf{r},t)\rangle + \Phi(\mathbf{r}',t)\langle\hat{\eta}^\dagger(\mathbf{r}',t)\hat{\eta}(\mathbf{r},t)\rangle \quad (2.11)$$

$$+\Phi(\mathbf{r},t)\langle\hat{\eta}^\dagger(\mathbf{r}',t)\hat{\eta}(\mathbf{r}',t)\rangle + \langle\hat{\eta}^\dagger(\mathbf{r}',t)\hat{\eta}(\mathbf{r}',t)\hat{\eta}(\mathbf{r},t)\rangle\Big].$$

So far the only approximation that has been made is the separation of the field operator into a classical field and a fluctuation operator. If all the terms including $\hat{\eta}$ are neglected we immediately obtain a mean-field equation in Φ known as the Gross-Pitaevskii equation [48–50]. To go one step further we keep in Eq. (2.11) terms with precisely two fluctuation operators, treating $\xi \sim \langle\hat{\eta}^\dagger\hat{\eta}\rangle/\langle\hat{\Psi}^\dagger\hat{\Psi}\rangle \sim \langle\hat{\eta}\hat{\eta}\rangle/\langle\hat{\Psi}^\dagger\hat{\Psi}\rangle$ as a small number. An equation of motion for $\hat{\eta}$ at this level of approximation can be found by subtracting Eq. (2.11) from Eq. (2.10), leading to

$$i\frac{\partial \hat{\eta}(\mathbf{r},t)}{\partial t} = h(\mathbf{r},t)\hat{\eta}(\mathbf{r},t) + \int d\mathbf{r}' V_{\text{int}}(\mathbf{r}'-\mathbf{r})\Big[|\Phi(\mathbf{r}',t)|^2\hat{\eta}(\mathbf{r},t)$$

$$+ \Phi^*(\mathbf{r}',t)\Phi(\mathbf{r},t)\hat{\eta}(\mathbf{r}',t) + \Phi(\mathbf{r}',t)\Phi(\mathbf{r},t)\hat{\eta}^\dagger(\mathbf{r}',t)\Big], \quad (2.12)$$

where in acquiring Eq. (2.12) it has been assumed that the fluctuations around the expectation values of the operators $\hat{\eta}^\dagger\hat{\eta}$ and $\hat{\eta}\hat{\eta}$ are small such that terms of the form $\hat{\eta}^\dagger\hat{\eta} - \langle\hat{\eta}^\dagger\hat{\eta}\rangle$ and $\hat{\eta}\hat{\eta} - \langle\hat{\eta}\hat{\eta}\rangle$ may be neglected. To proceed, the fluctuation operator is written as [51, 52]

$$\hat{\eta}(\mathbf{r},t) = \sum_i \Big[u_i(\mathbf{r},t)e^{-it\epsilon_i(t)}\hat{\alpha}_i + v_i^*(\mathbf{r},t)e^{it\epsilon_i^*(t)}\hat{\alpha}_i^\dagger \Big], \quad (2.13)$$

where the functions $u_i(\mathbf{r},t)$, $v_i(\mathbf{r},t)$ and $\epsilon_i(t)$ are assumed to vary slowly in time, treating the inclusion of quantum fluctuations in a quasi-static manner. The operators $\hat{\alpha}_i$ ($\hat{\alpha}_i^\dagger$) are bosonic annihilation (creation) operators such that $\hat{\alpha}_i$ annihilate the ground state of the system, corresponding to non-interacting bosonic quasi-particles with the energies ϵ_i. The commutation relations for the field operator $[\hat{\Psi}(\mathbf{r},t), \hat{\Psi}^\dagger(\mathbf{r}',t)] = \delta(\mathbf{r}'-\mathbf{r})$ and $[\hat{\Psi}(\mathbf{r},t), \hat{\Psi}(\mathbf{r}',t)] = 0$ together with the commutation relations for the quasi-particle operators $[\hat{\alpha}_i, \hat{\alpha}_j^\dagger] = \delta_{ij}$ and $[\hat{\alpha}_i, \hat{\alpha}_j] = 0$ impose the following relations on the amplitudes u_i and v_i [47]

$$\sum_i \left[u_i(\mathbf{r}', t) u_i^*(\mathbf{r}, t) - v_i^*(\mathbf{r}', t) v_i(\mathbf{r}, t) \right] = \delta(\mathbf{r}' - \mathbf{r})$$

$$\sum_i \left[u_i(\mathbf{r}', t) v_i^*(\mathbf{r}, t) - v_i^*(\mathbf{r}', t) u_i(\mathbf{r}, t) \right] = 0. \tag{2.14}$$

By substituting the form of the fluctuation operator in Eq. (2.13) into Eq (2.12) and comparing coefficients for the operators $\hat{\alpha}_i$ and $\hat{\alpha}_i^\dagger$ one obtains a system of integro-differential equations known as the Bogoliubov-de Gennes equations [51], which read

$$
\begin{aligned}
\left[\epsilon_i - h(\mathbf{r}) \right] u_i(\mathbf{r}) = \int \mathrm{d}\mathbf{r}'\, V_{\mathrm{int}}(\mathbf{r}' - \mathbf{r}) \Big[|\Phi(\mathbf{r}')|^2 u_i(\mathbf{r}) \\
+ \Phi^*(\mathbf{r}')\Phi(\mathbf{r}) u_i(\mathbf{r}') + \Phi(\mathbf{r}')\Phi(\mathbf{r}) v_i(\mathbf{r}') \Big] \\
\left[-\epsilon_i - h(\mathbf{r}) \right] v_i(\mathbf{r}) = \int \mathrm{d}\mathbf{r}'\, V_{\mathrm{int}}(\mathbf{r}' - \mathbf{r}) \Big[|\Phi(\mathbf{r}')|^2 v_i(\mathbf{r}) \\
+ \Phi(\mathbf{r}')\Phi^*(\mathbf{r}) v_i(\mathbf{r}') + \Phi^*(\mathbf{r}')\Phi^*(\mathbf{r}) u_i(\mathbf{r}') \Big],
\end{aligned}
\tag{2.15}
$$

where all time arguments have been omitted for notational clarity. In order to solve Eqs. (2.15) we make a series of approximations, starting with the semi-classical approximation [21, 22, 53] where the following replacements are made:

$$
\begin{aligned}
\epsilon_i &\rightarrow \epsilon(\mathbf{r}, \mathbf{k}) \\
q_i(\mathbf{r}) &\rightarrow q(\mathbf{r}, \mathbf{k}) \mathrm{e}^{\mathrm{i}\mathbf{k}\cdot\mathbf{r}} \\
\sum_i &\rightarrow \int \frac{\mathrm{d}\mathbf{k}}{(2\pi)^3}.
\end{aligned}
\tag{2.16}
$$

Here q, which stands for either u or v, is assumed to vary slowly with $\mathbf{r}$ such that the behavior of $q(\mathbf{r}, \mathbf{k})\mathrm{e}^{\mathrm{i}\mathbf{k}\cdot\mathbf{r}}$ is approximately that of a plane wave. Following this approximation the Bogoliubov-de Gennes equations no longer contain differential terms but still integral ones, which take the form

$$I(\mathbf{r}, \mathbf{k}) = \int \mathrm{d}\mathbf{r}'\, V_{\mathrm{int}}(\mathbf{r}')\mathrm{e}^{\mathrm{i}\mathbf{k}\cdot\mathbf{r}'} X(\mathbf{r} + \mathbf{r}') q(\mathbf{r} + \mathbf{r}', \mathbf{k}), \tag{2.17}$$

where X stands for either Φ or Φ^*. Motivated by the assumed slow variation of the involved functions, $X(\mathbf{r} + \mathbf{r}', \mathbf{k})q(\mathbf{r} + \mathbf{r}', \mathbf{k})$ is expanded around $\mathbf{r}$ such that the above integral can be written

$$I(\mathbf{r}, \mathbf{k}) = \tilde{V}_{\text{int}}(\mathbf{k})X(\mathbf{r})q(\mathbf{r}, \mathbf{k}) - i\nabla_{\mathbf{k}}\tilde{V}_{\text{int}}(\mathbf{k}) \cdot \nabla_{\mathbf{r}}\left[X(\mathbf{r})q(\mathbf{r}, \mathbf{k})\right] + \cdots, \quad (2.18)$$

where the Fourier transform of the interaction potential $\tilde{V}_{\text{int}}(\mathbf{k}) = \int d\mathbf{r}\, V_{\text{int}}(\mathbf{r})e^{-i\mathbf{k}\cdot\mathbf{r}}$ has been assumed to be symmetric in $\mathbf{k}$. In the local density approximation only the first term in Eq. (2.18) is kept, which is justified as long as [22]

$$\frac{\nabla_{\mathbf{k}}\tilde{V}_{\text{int}}(\mathbf{k}) \cdot \nabla_{\mathbf{r}}\left[X(\mathbf{r})q(\mathbf{r}, \mathbf{k})\right]}{\tilde{V}_{\text{int}}(\mathbf{k})X(\mathbf{r})q(\mathbf{r}, \mathbf{k})} \ll 1. \quad (2.19)$$

Finally, by using Eq. (2.11) the chemical potential potential in Eq. (2.15) is approximated according to

$$\mu \approx V_{\text{ext}}(\mathbf{r}) + \int d\mathbf{r}'\, V_{\text{int}}(\mathbf{r}' - \mathbf{r})|\Phi(\mathbf{r}')|^2, \quad (2.20)$$

where small terms including the fluctuation operator $\hat{\eta}$ have been neglected as well as any space and time derivatives of Φ, consistent with the above assumption that u and v are slowly-varying functions in space and time. The combination of all these approximations transforms Eqs. (2.15) into the linear form

$$\begin{pmatrix} T(\mathbf{r}, \mathbf{k}) & V(\mathbf{r}, \mathbf{k}) \\ -V^*(\mathbf{r}, \mathbf{k}) & -T(\mathbf{r}, \mathbf{k}) \end{pmatrix} \begin{pmatrix} u(\mathbf{r}, \mathbf{k}) \\ v(\mathbf{r}, \mathbf{k}) \end{pmatrix} = \epsilon(\mathbf{r}, \mathbf{k}) \begin{pmatrix} u(\mathbf{r}, \mathbf{k}) \\ v(\mathbf{r}, \mathbf{k}) \end{pmatrix}, \quad (2.21)$$

where $T(\mathbf{r}, \mathbf{k}) \equiv \mathbf{k}^2/2 + |\Phi(\mathbf{r})|^2 \tilde{V}_{\text{int}}(\mathbf{k})$ and $V \equiv [\Phi(\mathbf{r})]^2 \tilde{V}_{\text{int}}(\mathbf{k})$. The energy solution is

$$\epsilon(\mathbf{r}, \mathbf{k}) = \sqrt{\frac{\mathbf{k}^2}{2}\left[\frac{\mathbf{k}^2}{2} + 2|\Phi(\mathbf{r})|^2 \tilde{V}_{\text{int}}(\mathbf{k})\right]}, \quad (2.22)$$

and the amplitudes can be found by combining Eqs. (2.21) with the relations in Eq. (2.14), yielding

$$|u(\mathbf{r}, \mathbf{k})|^2 = \frac{\mathbf{k}^2/2 + |\Phi(\mathbf{r})|^2 \, \tilde{V}_{\text{int}}(\mathbf{k}) + \epsilon(\mathbf{r}, \mathbf{k})}{2\epsilon(\mathbf{r}, \mathbf{k})}$$

$$|v(\mathbf{r}, \mathbf{k})|^2 = \frac{\mathbf{k}^2/2 + |\Phi(\mathbf{r})|^2 \, \tilde{V}_{\text{int}}(\mathbf{k}) - \epsilon(\mathbf{r}, \mathbf{k})}{2\epsilon(\mathbf{r}, \mathbf{k})} \qquad (2.23)$$

$$u(\mathbf{r}, \mathbf{k})v^*(\mathbf{r}, \mathbf{k}) = -\frac{[\Phi(\mathbf{r})]^2 \, \tilde{V}_{\text{int}}(\mathbf{k})}{2\epsilon(\mathbf{r}, \mathbf{k})}.$$

At this point not much has been said about the two-body interaction potential V_{int}, and here we are interested in two types of interactions: short-range and dipolar. 'Short-range' refers to interactions where in the zero-energy limit only the s-wave contribution to the scattering amplitude is non-neglible such that the interaction can be characterized by a single number: the s-wave scattering length a_s. In three dimensions this is the case for potentials that go to zero faster than r^{-3} [24], and it is then possible to replace the true interaction potential with a pseudopotential of the form

$$V_{\text{pseudo}}(\mathbf{r}) = \lambda\delta(\mathbf{r}), \qquad (2.24)$$

where λ characterizes the strength of the short-range interaction. The second type of interaction that will be considered here is the dipole-dipole interaction, where the two-body potential for particles with dipole moments in the same direction is [54]

$$V_{\text{dd}}(\mathbf{r}) = \frac{C_{\text{dd}}}{4\pi|\mathbf{r}|^3} \left(1 - 3\cos^2\theta\right), \qquad (2.25)$$

where θ is the angle between the polarization direction and $\mathbf{r}$. The strength of the interaction C_{dd} is equal to $\mu_0\mu_{\text{dd}}^2$ for magnetic dipoles and $d_{\text{dd}}^2/\epsilon_0$ for electric dipoles, where μ_0 is the vacuum permeability, μ_{dd} the magnetic dipole moment, ϵ_0 the vacuum permittivity, and d_{dd} the electric dipole moment. Since V_{dd} goes to zero as r^{-3}, partial waves other than the s-wave contribute to the scattering amplitude even at low energies, and the interaction can consequently not be classified as short-range. Here, we will consider systems that have both these types of interactions, and the total two-body potential reads

$$V_{\text{int}}(\mathbf{r}) = \lambda\delta(\mathbf{r}) + \frac{C_{\text{dd}}}{4\pi|\mathbf{r}|^3}\left(1 - 3\cos^2\theta\right), \tag{2.26}$$

which has the Fourier transform [55]

$$\tilde{V}_{\text{int}}(\mathbf{k}) = \lambda + \frac{C_{\text{dd}}}{3}\left(3\cos^2\alpha - 1\right), \tag{2.27}$$

where α is the angle between $\mathbf{k}$ and the polarization direction. In a second-order Born approximation[2] the scattering amplitude in the low-energy limit for this potential reads [56]

$$f(\mathbf{k}\to 0) = -\frac{1}{4\pi}\tilde{V}_{\text{int}}(\mathbf{k}\to 0) + \frac{1}{4\pi}\int\frac{d\mathbf{q}}{(2\pi)^3}\frac{[\tilde{V}_{\text{int}}(\mathbf{q})]^2}{q^2}. \tag{2.28}$$

The total scattering length, defined as $a \equiv -f(\mathbf{k}\to 0)$, is dependent on the direction of the limit $\mathbf{k}\to 0$ due to the anisotropy of the dipole-dipole interaction. By separating the scattering length into a sum of the isotropic s-wave part a_s and an anisotropic part corresponding to the rest of the partial waves, the s-wave scattering length can be identified as [22]

$$a_s = \frac{\lambda}{4\pi} - \frac{1}{4\pi}\int\frac{d\mathbf{k}}{(2\pi)^3}\frac{[\tilde{V}_{\text{int}}(\mathbf{k})]^2}{k^2}. \tag{2.29}$$

It is at this point useful to define the coupling constants $g \equiv 4\pi a_s$ and $g_{\text{dd}} \equiv C_{\text{dd}}/3$, as well as the relative interaction strength $\varepsilon_{\text{dd}} \equiv g_{\text{dd}}/g$. By using the solutions to the Bogoliubov-de Gennes equations in Eq. (2.22) and Eq. (2.23) the equation of motion for the order parameter can now be written

$$i\frac{\partial\Phi(\mathbf{r}, t)}{\partial t} = \left[h(\mathbf{r}, t) + gn(\mathbf{r}, t) + \int d\mathbf{r}' V_{\text{dd}}(\mathbf{r}' - \mathbf{r})n(\mathbf{r}', t)\right.$$
$$\left. + \frac{4g^{5/2}}{3\pi^2}\mathcal{Q}_5(\varepsilon_{\text{dd}})n(\mathbf{r}, t)^{3/2}\right]\Phi(\mathbf{r}, t), \tag{2.30}$$

---

[2]It is here necessary to use a second-order approximation in order to avoid a divergence at high momenta when calculating an integral needed to obtain the equation of motion in Eq. (2.30).

where $n(\mathbf{r}, t) \equiv \langle \hat{\Psi}^\dagger(\mathbf{r}, t)\hat{\Psi}(\mathbf{r}, t)\rangle$ is the total density, subject to the normalization condition $N = \int \mathrm{d}\mathbf{r}\, n$ which reads

$$N = \int \mathrm{d}\mathbf{r} \left[|\Phi(\mathbf{r}, t)|^2 + \frac{g^{3/2}}{3\pi^2} \mathcal{Q}_3(\varepsilon_{\mathrm{dd}})|\Phi(\mathbf{r}, t)|^3 \right]. \qquad (2.31)$$

The functions $\mathcal{Q}_3(\varepsilon_{\mathrm{dd}})$ and $\mathcal{Q}_5(\varepsilon_{\mathrm{dd}})$ come from the polar-angle part of the momentum integration and are defined as

$$\mathcal{Q}_l(\varepsilon_{\mathrm{dd}}) = \int_0^1 \mathrm{d}u \left[1 + \varepsilon_{\mathrm{dd}}(3u^2 - 1) \right]^{l/2}. \qquad (2.32)$$

The quantum depletion density, which by assumption is small, is equal to [21, 22]

$$\frac{\langle \hat{\eta}^\dagger(\mathbf{r}, t)\hat{\eta}(\mathbf{r}, t)\rangle}{n(\mathbf{r}, t)} = \frac{\sqrt{n(\mathbf{r}, t)g^3}}{3\pi^2} \mathcal{Q}_3(\varepsilon_{\mathrm{dd}}), \qquad (2.33)$$

revealing $\sqrt{ng^3}$ as the relevant small parameter of the system. The function $\mathcal{Q}_l(\varepsilon_{\mathrm{dd}})$ has a non-zero imaginary part for $\varepsilon_{\mathrm{dd}} > 1$, which is a consequence of the modes in Eq. (2.22) becoming imaginary at low energies for large values of the relative interaction strength. As long as $\varepsilon_{\mathrm{dd}}$ is not too large this imaginary part is small compared to the real part, see Fig. 2.1 for an example with $\mathcal{Q}_5(\varepsilon_{\mathrm{dd}})$, and in calculations involving Eq. (2.30) it is typically ignored, see for example Refs. [30–34]. An alternative way to treat the last term in Eq. (2.30) is by expanding $\mathcal{Q}_5(\varepsilon_{\mathrm{dd}})$ for small $\varepsilon_{\mathrm{dd}}$ according to [31, 57]

$$\mathcal{Q}_5(\varepsilon_{\mathrm{dd}}) = 1 + \frac{3}{2}\varepsilon_{\mathrm{dd}}^2 + \frac{1}{7}\varepsilon_{\mathrm{dd}}^3 - \frac{3}{56}\varepsilon_{\mathrm{dd}}^4 + \mathcal{O}(\varepsilon_{\mathrm{dd}}^5), \qquad (2.34)$$

and then keep terms up to some order in $\varepsilon_{\mathrm{dd}}$. Although using a small-value expansion for $\mathcal{Q}_5(\varepsilon_{\mathrm{dd}})$ when $\varepsilon_{\mathrm{dd}} > 1$ may not seem like a sound idea, it can be seen from Fig. 2.1 that the relative difference compared to $\mathrm{Re}\{\mathcal{Q}_5(\varepsilon_{\mathrm{dd}})\}$ is not too large for small enough $\varepsilon_{\mathrm{dd}}$. It should be noted that it is customary when working with Eq. (2.30) to make the replacement $n \to |\Phi|^2$. This may at first glance seem strange since equating the total density and the condensate density is equivalent
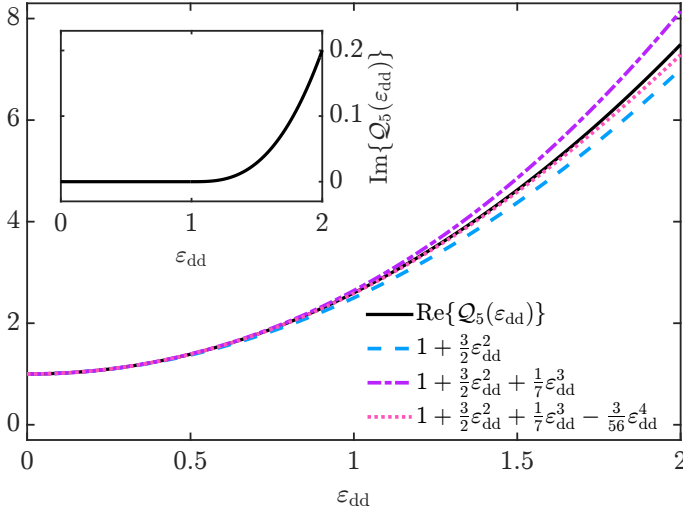
Figure 2.1: The function $\mathcal{Q}_5(\varepsilon_{dd})$ as a function of ε_{dd}, where the main figure shows the real part of $\mathcal{Q}_5(\varepsilon_{dd})$ as well as some approximations to different orders in ε_{dd} according to Eq. (2.34), and the inset shows the imaginary part of $\mathcal{Q}_5(\varepsilon_{dd})$.

to setting $\langle \hat{\eta}^\dagger \hat{\eta} \rangle = 0$, leading to the mean-field formalism where quantum fluctuations are not taken into account. However, because we are usually not interested in the (small) difference between n and $|\Phi|^2$ per se, but rather in the effects of incorporating higher order terms, such a replacement can be motivated as long as the quantum depletion is small. In order to obtain the energy of the system one can diagonalize the grand-canonical Hamiltonian using the techniques and approximations outlined in this section [21, 22]. Alternatively, following the replacement $n \to |\Phi|^2$ in Eq. (2.30), the energy can be obtained simply by finding the action for which this equation of motion is the corresponding Euler-Lagrange equation. Equation (2.30) is often referred to as an "extended" Gross-Pitaevskii equation, and serves as the basis for our studies in Paper II.

The last term in Eq. (2.30) is positive, and implies a more strongly repulsive interaction compared to the mean-field picture. This additional repulsion can counteract the attractive part of the dipole-dipole interaction and extend the stability region of the system such that Eq. (2.30) may lead to droplet solutions [30–34]. These droplets can exist as a stable configurations without external trapping, and have been confirmed both experimentally [26–29] and by using for example Monte-Carlo methods [58, 59].

Finally, due to the intimate connection between Bose-Einstein condensation and superfluidity, we are interested in systems with rotating confinements, which are most easily studied in the frame that rotates with the external potential. If $|\Psi\rangle$ is a solution to the Schrödinger equation with the Hamiltonian $\hat{H}$, then the state ket $e^{it\Omega\hat{L}_z}|\Psi\rangle$ rotated by an angle $-t\Omega$ around the z-axis obeys the Schrödinger equation with the Hamiltonian $\hat{H} - \Omega\hat{L}_z$, where $\hat{L}_z$ is the z-component of the angular momentum operator. Now, assuming that the interaction terms in the extended Gross-Pitaevskii equation Eq. (2.30) are unchanged under rotation, the corresponding equations in the rotating frame are obtained by adding $-\Omega L_z$ to the right-hand side of these equations, where $L_z = \mathrm{i}(y\partial_x - x\partial_y)$. Bosonic configurations in rotating trapping potentials are investigated in Papers I, II, and IV.

2.3   Bose-Bose Mixtures with Short-Range Interactions

We now consider binary Bose mixtures in the specific case where the particle masses of both components are equal and the interactions are exclusively short-range. For a mixture with N_σ particles in component σ and interactions between components σ and σ' characterized by the constants $\lambda_{\sigma\sigma'}$ the Hamiltonian is

$$
\begin{aligned}
\hat{H} = \sum_\sigma \int \mathrm{d}\mathbf{r}\, \hat{\Psi}_\sigma^\dagger(\mathbf{r}, t) h_0(\mathbf{r}, t) \hat{\Psi}_\sigma(\mathbf{r}, t) \\
+ \frac{1}{2} \sum_{\sigma\sigma'} \int \mathrm{d}\mathbf{r}\, \lambda_{\sigma\sigma'} \hat{\Psi}_{\sigma'}^\dagger(\mathbf{r}, t) \hat{\Psi}_\sigma^\dagger(\mathbf{r}, t) \hat{\Psi}_{\sigma'}(\mathbf{r}, t) \hat{\Psi}_\sigma(\mathbf{r}, t),
\end{aligned}
\tag{2.35}
$$

where it has been assumed that the different components are affected by the same external potential. We will for these mixtures also be interested in dimensionally reduced systems, and the position and momentum vectors are to be understood as D-dimensional, where $D = 1, 2, 3$. The Heisenberg equations of motion with respect to the grand-canonical Hamiltonian $\hat{K} = \hat{H} - \sum_\sigma \mu_\sigma \hat{N}_\sigma$ is

$$
\mathrm{i}\frac{\partial \hat{\Psi}_\sigma(\mathbf{r}, t)}{\partial t} = h_\sigma(\mathbf{r}, t) \hat{\Psi}_\sigma(\mathbf{r}, t) + \sum_{\sigma'} \lambda_{\sigma\sigma'} \hat{\Psi}_{\sigma'}^\dagger(\mathbf{r}, t) \hat{\Psi}_{\sigma'}(\mathbf{r}, t) \hat{\Psi}_\sigma(\mathbf{r}, t), \tag{2.36}
$$

where $\hat{N}_\sigma$ is the number operator for component σ, μ_σ the chemical potential for component σ, and $h_\sigma(\mathbf{r}, t) \equiv h_0(\mathbf{r}, t) - \mu_\sigma(t)$. The relevant small number ξ is like in the previous section the quantum depletion density $\xi \sim \langle \hat{\eta}_\sigma^\dagger \hat{\eta}_\sigma \rangle / \langle \hat{\Psi}_\sigma^\dagger \hat{\Psi}_\sigma \rangle$. The equations of motion for the order parameters Φ_σ can be found following the procedure described for the single-component Bose system. The field operators are separated according to

$$\hat{\Psi}_\sigma(\mathbf{r}, t) = \Phi_\sigma(\mathbf{r}, t) + \hat{\eta}_\sigma(\mathbf{r}, t), \tag{2.37}$$

where the fluctuation operators are now written as

$$
\begin{aligned}
\hat{\eta}_1(\mathbf{r}, t) = \sum_i \Big[& a_{1,i}(\mathbf{r}, t)e^{-it\epsilon_{\alpha,i}(t)}\hat{\alpha}_i + a_{2,i}^*(\mathbf{r}, t)e^{it\epsilon_{\alpha,i}^*(t)}\hat{\alpha}_i^\dagger \\
& + b_{1,i}(\mathbf{r}, t)e^{-it\epsilon_{\beta,i}(t)}\hat{\beta}_i + b_{2,i}^*(\mathbf{r}, t)e^{it\epsilon_{\beta,i}^*(t)}\hat{\beta}_i^\dagger \Big] \\
\hat{\eta}_2(\mathbf{r}, t) = \sum_i \Big[& a_{3,i}(\mathbf{r}, t)e^{-it\epsilon_{\alpha,i}(t)}\hat{\alpha}_i + a_{4,i}^*(\mathbf{r}, t)e^{it\epsilon_{\alpha,i}^*(t)}\hat{\alpha}_i^\dagger \\
& + b_{3,i}(\mathbf{r}, t)e^{-it\epsilon_{\beta,i}(t)}\hat{\beta}_i + b_{4,i}^*(\mathbf{r}, t)e^{it\epsilon_{\beta,i}^*(t)}\hat{\beta}_i^\dagger \Big].
\end{aligned}
\tag{2.38}
$$

Unlike the single-component case there are now two types of bosonic quasi-particle operators $\hat{\alpha}_i$ and $\hat{\beta}_i$ with the respective energies $\epsilon_{\alpha,i}$ and $\epsilon_{\beta,i}$. Under the same approximations as for the one-component case we are lead to linear systems of equations $\mathbf{Ma} = \epsilon_\alpha \mathbf{a}$ and $\mathbf{Mb} = \epsilon_\beta \mathbf{b}$, with $\mathbf{a} = \begin{pmatrix} a_1 & a_2 & a_3 & a_4 \end{pmatrix}^\mathrm{T}$, $\mathbf{b} = \begin{pmatrix} b_1 & b_2 & b_3 & b_4 \end{pmatrix}^\mathrm{T}$, and

$$
\mathbf{M} = \begin{pmatrix}
T_1(\mathbf{r}, \mathbf{k}, t) & V_1(\mathbf{r}, t) & W_{12}(\mathbf{r}, t) & V_{12}(\mathbf{r}, t) \\
-V_1^*(\mathbf{r}, t) & -T_1(\mathbf{r}, \mathbf{k}, t) & -V_{12}^*(\mathbf{r}, t) & -W_{12}^*(\mathbf{r}, t) \\
W_{12}^*(\mathbf{r}, t) & V_{12}(\mathbf{r}, t) & T_2(\mathbf{r}, \mathbf{k}, t) & V_2(\mathbf{r}, t) \\
-V_{12}^*(\mathbf{r}, t) & -W_{12}(\mathbf{r}, t) & -V_2^*(\mathbf{r}, t) & -T_2(\mathbf{r}, \mathbf{k}, t)
\end{pmatrix}, \tag{2.39}
$$

where $T_i(\mathbf{r}, \mathbf{k}, t) \equiv \mathbf{k}^2/2 + \lambda_{ii}|\Phi_i(\mathbf{r}, t)|^2$, $V_i(\mathbf{r}, t) \equiv \lambda_{ii}[\Phi_i(\mathbf{r}, t)]^2$, $V_{12}(\mathbf{r}, t) \equiv \lambda_{12}\Phi_1(\mathbf{r}, t)\Phi_2(\mathbf{r}, t)$, and $W_{12}(\mathbf{r}, t) \equiv \lambda_{12}\Phi_1(\mathbf{r}, t)\Phi_2^*(\mathbf{r}, t)$. The energy solutions are [20, 23]

$$\epsilon_\pm(\mathbf{r}, \mathbf{k}, t) = \sqrt{\frac{\mathbf{k}^2}{2}\left[\frac{\mathbf{k}^2}{2} + 2c_\pm^2(\mathbf{r}, t)\right]}, \qquad (2.40)$$

where

$$2c_\pm^2(\mathbf{r}, t) = \lambda_{11}|\Phi_1(\mathbf{r}, t)|^2 + \lambda_{22}|\Phi_2(\mathbf{r}, t)|^2$$
$$\pm \sqrt{\left(\lambda_{11}|\Phi_1(\mathbf{r}, t)|^2 - \lambda_{22}|\Phi_2(\mathbf{r}, t)|^2\right)^2 + 4\lambda_{12}^2|\Phi_1(\mathbf{r}, t)|^2|\Phi_2(\mathbf{r}, t)|^2}. \qquad (2.41)$$

Note that the energies ϵ_α and ϵ_β can not be equal to the same energy branch $\epsilon_\pm$ if the bosonic commutation relations for $\hat{\Psi}_\sigma$, $\hat{\alpha}_i$ and $\hat{\beta}_i$ are to be satisfied. Here we focus on the parameter regime where the intraspecies coupling constants $\lambda_{\sigma\sigma}$ are positive and

$$\frac{\lambda_{12}^2}{\lambda_{11}\lambda_{22}} \sim 1 + \mathcal{O}(\xi). \qquad (2.42)$$

In this regime the equations of motion for the order parameters are

$$i\frac{\partial\Phi_\sigma(\mathbf{r}, t)}{\partial t} = \left\{ h_\sigma(\mathbf{r}, t) + \lambda_{\sigma\sigma}n_\sigma(\mathbf{r}, t) + \lambda_{\sigma\sigma'}n_{\sigma'}(\mathbf{r}, t) \right.$$
$$\left. + \frac{\lambda_{\sigma\sigma}}{2}\int\frac{d\mathbf{k}}{(2\pi)^D}\left[\frac{\mathbf{k}^2/2 - \epsilon_+(\mathbf{r}, \mathbf{k}, t)}{\epsilon_+(\mathbf{r}, \mathbf{k}, t)}\right] \right\}\Phi_\sigma(\mathbf{r}, t), \qquad (2.43)$$

where it is implied that $\sigma \neq \sigma'$ and $n_\sigma(\mathbf{r}, t) \equiv \langle\hat{\Psi}_\sigma^\dagger(\mathbf{r}, t)\hat{\Psi}_\sigma(\mathbf{r}, t)\rangle$ is subject to the normalization condition $N_\sigma = \int d\mathbf{r}\, n_\sigma$. We see that Eqs. (2.43) are independent of ϵ_- to lowest non-vanishing order in ξ under the condition in Eq. (2.42). These modes become imaginary for small $\mathbf{k}$ when $\lambda_{12}^2 > \lambda_{11}\lambda_{22}$, and the neglect of these modes is analogous to the dipolar case where the imaginary part of $\mathcal{Q}_5(\varepsilon_{dd})$ was ignored.

2.3.1 Binary Bose Mixtures in Three Dimensions

In three dimensions the coupling constants are expressed in terms of the s-wave scattering length through a second-order Born approximation [56]

$$\lambda_{\sigma\sigma'} = g_{\sigma\sigma'} \left[1 + \int \frac{\mathrm{d}\mathbf{k}}{(2\pi)^3} \frac{g_{\sigma\sigma'}}{k^2} \right], \qquad (2.44)$$

where $g_{\sigma\sigma'} \equiv 4\pi a_{\sigma\sigma'}$ and $a_{\sigma\sigma'}$ is the s-wave scattering length for the interaction between components σ and σ'. The momentum integration in Eqs. (2.43) then results in

$$
i\frac{\partial \Phi_\sigma(\mathbf{r}, t)}{\partial t} = \Bigg\{ h_\sigma(\mathbf{r}, t) + g_{\sigma\sigma} n_\sigma(\mathbf{r}, t) + g_{\sigma\sigma'} n_{\sigma'}(\mathbf{r}, t)
$$
$$
+ \frac{4 g_{\sigma\sigma}}{3\pi^2} \left[g_{11} n_1(\mathbf{r}, t) + g_{22} n_2(\mathbf{r}, t) \right]^{3/2} \Bigg\} \Phi_\sigma(\mathbf{r}, t), \qquad (2.45)
$$

and the quantum depletion density is in this case

$$\frac{\langle \hat{\eta}_\sigma^\dagger(\mathbf{r}, t) \hat{\eta}_\sigma(\mathbf{r}, t) \rangle}{n_\sigma(\mathbf{r}, t)} = \frac{g_{\sigma\sigma} \sqrt{g_{11} n_1(\mathbf{r}, t) + g_{22} n_2(\mathbf{r}, t)}}{3\pi^2}. \qquad (2.46)$$

Consider now for simplicity a uniform symmetric system without external trapping where $g_{\sigma\sigma} = g$ and $n_\sigma = n$ in the regime where $\delta g \equiv g_{12} + g \sim \mathcal{O}(\xi)$ and $\delta g < 0$. The energy density is then $\delta g n^2 + 32\sqrt{2}(gn)^{5/2}/(15\pi^2)$, where the two terms are of the same order of magnitude, have opposite signs, and depend differently on the density, leading to an energy that is minimized at a finite density. This type of finite-density minimization can, much like in the dipolar case, lead to self-bound droplet states [23]. Interestingly, as an alternative mechanism leading to quantum droplets, it has also been suggested that the inclusion of three-body interactions can result in such self-bound configurations in systems with short-range interactions [60]. If we instead flip the sign of the interparticle interaction coupling constant g_{12} and consider the regime where $g_{12} \sim \sqrt{g_{11} g_{22}} + \mathcal{O}(\xi)$, i.e.

close to the miscibility-immiscibility transition, it is found that the beyond mean-field contribution can lead to a new phase where mixed and pure phases coexist [39].

2.3.2 Binary Bose Mixtures in Two Dimensions

In two dimensions the integral in Eq. (2.43) diverges for large momenta and it is necessary to introduce a cutoff κ, corresponding to letting the short-range interaction constants be zero for momenta above this value. The coupling constants are then related to the two-dimensional scattering lengths $a_{\sigma\sigma'}^{\text{2d}}$ according to [61]

$$\lambda_{\sigma\sigma'} = \frac{4\pi}{\ln\left(\epsilon_{\sigma\sigma'}/\kappa^2\right)} \equiv g_{\sigma\sigma'}, \tag{2.47}$$

where $\epsilon_{\sigma\sigma'} = 4e^{-2\gamma}/(a_{\sigma\sigma'}^{\text{2d}})^2$ and γ is Euler's constant. If the transversal trap is harmonic with a confinement length l these two-dimensional scattering lengths can be expressed in terms of the three-dimensional ones $a_{\sigma\sigma'}$ through the relation

$$a_{\sigma\sigma'}^{\text{2d}} = l\sqrt{\frac{\pi}{B}} \exp\left(-\sqrt{\frac{\pi}{2}}\frac{l}{a_{\sigma\sigma'}}\right), \tag{2.48}$$

where $B \approx 0.915$ [62]. The asymptotic form of the equations of motion for the two-dimensional system in the limit $\kappa \gg \sqrt{g_{11}n_1 + g_{22}n_2}$ can now be written

$$\begin{aligned}
i\frac{\partial\Phi_\sigma(\mathbf{r},t)}{\partial t} &= \left\{ h_\sigma(\mathbf{r},t) + g_{\sigma\sigma}n_\sigma(\mathbf{r},t) + g_{\sigma\sigma'}n_{\sigma'}(\mathbf{r},t) \right. \\
&\left. + \frac{g_{\sigma\sigma}}{4\pi}\left[g_{11}n_1(\mathbf{r},t) + g_{22}n_2(\mathbf{r},t)\right]\ln\left(\frac{e\left[g_{11}n_1(\mathbf{r},t) + g_{22}n_2(\mathbf{r},t)\right]}{\kappa^2}\right)\right\}\Phi_\sigma(\mathbf{r},t),
\end{aligned} \tag{2.49}$$

and the quantum depletion density is

$$\frac{\langle\hat{\eta}_\sigma^\dagger(\mathbf{r},t)\hat{\eta}_\sigma(\mathbf{r},t)\rangle}{n_\sigma(\mathbf{r},t)} = \frac{g_{\sigma\sigma}}{4\pi}, \tag{2.50}$$

which is independent of any particle densities. By introducing new coupling constants $\tilde{g}_{\sigma\sigma'} = 4\pi/\ln(\epsilon_{\sigma\sigma'}/\Delta)$ such that $\tilde{g}_{11}\tilde{g}_{22} = \tilde{g}_{12}^2$, it is found that the energy Δ must be [61]

$$\Delta = \sqrt{\epsilon_{12}\sqrt{\epsilon_{11}\epsilon_{22}}} \exp\left[-\frac{\ln^2\left(\epsilon_{11}/\epsilon_{22}\right)}{4\ln\left(\epsilon_{11}\epsilon_{22}/\epsilon_{12}^2\right)}\right]. \tag{2.51}$$

The coupling constants $g_{\sigma\sigma'}$ and $\tilde{g}_{\sigma\sigma'}$ are related according to

$$g_{\sigma\sigma'} = \tilde{g}_{\sigma\sigma'} + \frac{\tilde{g}_{\sigma\sigma'}^2}{4\pi}\ln\left(\frac{\kappa^2}{\Delta}\right) + \mathcal{O}(\tilde{g}_{\sigma\sigma'}^3), \tag{2.52}$$

and by substituting this expression for $g_{\sigma\sigma'}$ into Eq. (2.49) up to second order in $\tilde{g}_{\sigma\sigma'}$ we obtain the equations

$$
\begin{aligned}
i\frac{\partial\Phi_\sigma(\mathbf{r},t)}{\partial t} = &\left\{ h_\sigma(\mathbf{r},t) + \tilde{g}_{\sigma\sigma}n_\sigma(\mathbf{r},t) + \mathrm{sgn}(\tilde{g}_{12})\sqrt{\tilde{g}_{11}\tilde{g}_{22}}\,n_{\sigma'}(\mathbf{r},t) \right. \\
&\left. + \frac{\tilde{g}_{\sigma\sigma}}{4\pi}\left[\tilde{g}_{11}n_1(\mathbf{r},t) + \tilde{g}_{22}n_2(\mathbf{r},t)\right]\ln\left(\frac{e\left[\tilde{g}_{11}n_1(\mathbf{r},t) + \tilde{g}_{22}n_2(\mathbf{r},t)\right]}{\Delta}\right)\right\}\Phi_\sigma(\mathbf{r},t),
\end{aligned}
\tag{2.53}
$$

independent of the cutoff momentum κ. Now, as long as κ^2/Δ is not exponentially large $g_{\sigma\sigma'} \approx \tilde{g}_{\sigma\sigma'}$ and the two sets of coupling constants can be used interchangeably. The two-dimensional extended Gross-Pitaevskii equations for binary Bose mixtures with short-range interactions Eqs. (2.53) are used in both Paper I and Paper III.

2.3.3 Binary Bose Mixtures in One Dimensions

In one dimension, under the assumption that the transversal trapping is harmonic with a confinement length l that is much larger than the three-dimensional scattering lengths $a_{\sigma\sigma'}$, the coupling constants are related to the one-dimensional scattering lengths $a_{\sigma\sigma'}^{\mathrm{1d}}$ according to [63]

$$\lambda_{\sigma\sigma'} = -\frac{2}{a_{\sigma\sigma'}^{\mathrm{1d}}} \equiv g_{\sigma\sigma'}, \tag{2.54}$$

where $a_{\sigma\sigma'}^{\mathrm{1d}} = -l^2/(2a_{\sigma\sigma'})$. The equations of motion in one dimension are then

$$i\frac{\partial \Phi_\sigma(x,t)}{\partial t} = \left\{ h_\sigma(x,t) + g_{\sigma\sigma} n_\sigma(x,t) + g_{\sigma\sigma'} n_{\sigma'}(x,t) \right.$$
$$\left. - \frac{g_{\sigma\sigma}}{\pi} \left[g_{11} n_1(x,t) + g_{22} n_2(x,t) \right]^{1/2} \right\} \Phi_\sigma(x,t). \tag{2.55}$$

Interestingly, the last term in Eqs. (2.55) is in one dimension negative, leading to droplet formation in the regime where $g_{12} > -\sqrt{g_{11}g_{22}}$ [61, 64], in contrast to the situation in three dimensions where droplets can exist for $g_{12} < -\sqrt{g_{11}g_{22}}$ [23]. The quantum depletion density is

$$\frac{\langle \hat{\eta}_\sigma^\dagger(x,t)\hat{\eta}_\sigma(x,t)\rangle}{n_\sigma(x,t)} = \frac{g_{\sigma\sigma}}{2\pi\sqrt{g_{11}n_1(x,t) + g_{22}n_2(x,t)}} \int_0^\infty d\chi \left[\frac{\chi^2 + 2}{\chi\sqrt{\chi^2 + 4}} - 1 \right], \tag{2.56}$$

where the integral in $\chi \equiv k/\sqrt{g_{11}n_1 + g_{22}n_2}$ is divergent, i.e. strictly speaking there is no condensate. This does not necessarily mean that all is lost, and it has been shown that this type of analysis that uses an order parameter to describe the system can be applied also in one dimension [65]. If we introduce a lower-momentum cutoff $\kappa \sim 1/L$ to the integral in Eq. (2.56), where L is the spatial extent of the system, we find that

$$\frac{\langle \hat{\eta}_\sigma^\dagger(x,t)\hat{\eta}_\sigma(x,t)\rangle}{n_\sigma(x,t)} \approx \frac{g_{\sigma\sigma}}{2\pi\sqrt{g_{11}n_1(x,t) + g_{22}n_2(x,t)}} \left[\ln 4 - 2 - \ln \chi_c(x,t) \right], \tag{2.57}$$

where it has been assumed that $\chi_c \equiv \kappa/\sqrt{g_{11}n_1 + g_{22}n_2} \ll 1$. For similar orders of magnitude $n_1 \sim n_2 \sim n$ and $g_{11} \sim g_{22} \sim g$ the small number in one dimension

thus scales as $\sqrt{g/n}$, meaning that this type of formalism requires a sufficiently *high* density to be valid. Equations (2.55) for one-dimensional Bose-Bose mixtures with short-range interactions are taken as the model equations of motion in Paper IV.

Chapter 3

Superfluidity

What's in a name? That which we call a superfluid by any other name would flow as frictionlessly. The term 'superfluidity' holds promises of exotic physics, but what does it really imply? This chapter does not attempt to answer this question in full generality, but instead introduces a few basic concepts of superfluidity relevant to this thesis in the context of cold atomic gases.

3.1 Putting the Super in Superfluidity

Superfluidity can refer to a whole class of physical effects such as frictionless flow [6, 7], non-classical rotational inertia [66], or metastable persistent flow [67, 68]. We first consider a uniform Bose fluid consisting of N particles flowing through a tube with velocity $-\mathbf{v}$. If, in the frame where the fluid is at rest, the ground state energy is E_0 and the total momentum is zero, then the energy in the frame where the tube is stationary can be obtained through a Galilean transformation and is

$$E_1 = E_0 + \frac{N\mathbf{v} \cdot \mathbf{v}}{2}. \tag{3.1}$$

Consider now the addition of a single quasi-particle excitation with momentum $\mathbf{k}$ and energy $\epsilon(\mathbf{k})$. The energy in the fluid frame is then $E_0 + \epsilon(\mathbf{k})$, which leads to an energy in the tube frame equal to

$$E_2 = E_0 + \epsilon(\mathbf{k}) - \mathbf{v} \cdot \mathbf{k} + \frac{N\mathbf{v} \cdot \mathbf{v}}{2}. \tag{3.2}$$

The system with a single elementary excitation is energetically favorable when $E_2 < E_1$, i.e. when $\epsilon(\mathbf{k}) - \mathbf{v} \cdot \mathbf{k} < 0$. For isotropic $\epsilon(\mathbf{k})$ this energy is minimized whenever $\mathbf{v}$ and $\mathbf{k}$ are parallel, leading to the Landau critical velocity [69]

$$v_c = \min_k \frac{\epsilon(k)}{k}, \tag{3.3}$$

below which there can be no degradation of the fluid by means of quasi-particle excitations. As an example, we take the excitation spectrum in Eq. (2.22) of the one-component system studied in the previous chapter. For purely short-range interactions we have $\epsilon(k) = \sqrt{k^4/4 + k^2 g n_0}$, where n_0 is the condensate density, and the critical velocity is consequently $v_c = \sqrt{g n_0}$. A condensate of this type can thus can flow through a tube without losing energy through the creation of quasi-particles as long as the velocity is sufficiently low[1].

It is possible to take the above thought experiment further by imagining the fluid to consist of a normal part and a superfluid part [69, 70]. The normal component is assumed to flow as regular fluid and is thus dragged along the tube whereas the superfluid component is unaffected. We write the total density as $n = n_s + n_n$, which defines the superfluid density n_s in terms of the normal-component density n_n and the total density n. If the superfluid again flows with the velocity $-\mathbf{v}$ relative to the tube then the momentum density in the frame where the superfluid is stationary is equal to

$$n_n \mathbf{v} = \int \frac{d\mathbf{k}}{(2\pi)^3} N_\mathbf{v}(\mathbf{k}) \, \mathbf{k}, \tag{3.4}$$

where

$$N_\mathbf{v}(\mathbf{k}) = \frac{1}{e^{\beta[\epsilon(\mathbf{k}) - \mathbf{v} \cdot \mathbf{k}]} - 1} \tag{3.5}$$

---

[1]Note that there can, however, be other types of excitations such as vortices.

is the distribution of normal-component particles in the frame where the tube is stationary and $\epsilon(\mathbf{k})$ the energy of these particles in the frame where superfluid is stationary. If the velocity is small in the sense $\beta \mathbf{v} \cdot \mathbf{k} \ll 1$, we find for isotropic $\epsilon(\mathbf{k})$ that the normal density is

$$n_n = -\frac{1}{6\pi^2} \int_0^\infty \mathrm{d}k\, k^4 \frac{\mathrm{d}N_0}{\mathrm{d}\epsilon}. \tag{3.6}$$

For the one-component system with repulsive short-range interactions at low temperatures such that only energies $\epsilon(k) \approx k\sqrt{gn_0}$ contribute significantly, we obtain the normal density

$$n_n = \frac{2\pi^2 T^4}{45(gn_0)^{5/2}}, \tag{3.7}$$

revealing that the entire system becomes superfluid as the temperature goes to zero in this case. Crucially, the superfluid density is not the same as the condensate density (see for example Ref. [71]), and at low temperatures superfluid helium has as an example a superfluid fraction equal to one while the condensate fraction is around 0.1 [24].

3.2   Quantization of Circulation and Vortices

A fundamental property of superfluids is that they flow irrotationally [72], and to investigate this property in the context of Bose-Einstein condensation we start by taking the time derivative of $|\Phi(\mathbf{r}, t)|^2$ and use Eq. (2.55), resulting in

$$\frac{\partial |\Phi(\mathbf{r}, t)|^2}{\partial t} + \frac{i}{2}\nabla \cdot \left[\Phi(\mathbf{r}, t)\nabla \Phi^*(\mathbf{r}, t) - \Phi^*(\mathbf{r}, t)\nabla \Phi(\mathbf{r}, t)\right] = 0. \tag{3.8}$$

This has the form of a continuity equation

$$\frac{\partial n_0(\mathbf{r}, t)}{\partial t} + \nabla \cdot [n_0(\mathbf{r}, t)\mathbf{v}_0(\mathbf{r}, t)] = 0, \tag{3.9}$$

where $n_0(\mathbf{r}, t) \equiv |\Phi(\mathbf{r}, t)|^2$ is the condensate density and

$$\mathbf{v}_0(\mathbf{r}, t) \equiv \frac{i}{2|\Phi(\mathbf{r}, t)|^2} \left[\Phi(\mathbf{r}, t) \nabla \Phi^*(\mathbf{r}, t) - \Phi^*(\mathbf{r}, t) \nabla \Phi(\mathbf{r}, t) \right] \qquad (3.10)$$

the condensate velocity. By writing the order parameter in terms of an amplitude and a phase $\Phi(\mathbf{r}, t) = |\Phi(\mathbf{r}, t)| e^{i\phi(\mathbf{r}, t)}$ this velocity takes the form

$$\mathbf{v}_0(\mathbf{r}, t) = \nabla \phi(\mathbf{r}, t), \qquad (3.11)$$

showing that the condensate flow as defined in Eq. (3.10) is indeed irrotational. A consequence of this, together with the requirement that the order parameter has to be single valued, is that the circulation κ is quantized,

$$\kappa = \oint \mathbf{v}_0 \cdot d\mathbf{l} = 2\pi s, \qquad (3.12)$$

where the integer s is the winding number. For cylindrically symmetric flow only in the $\mathbf{e}_\varphi$ direction this implies the velocity field

$$\mathbf{v}_0 = \frac{s}{\rho} \mathbf{e}_\varphi, \qquad (3.13)$$

which for $s \neq 0$ diverges at $\rho = 0$, and the density thus has to go to zero at these points such that the flow takes the form of a vortex line. From Stokes' theorem it can be seen that the rotation of this velocity field is $\nabla \times \mathbf{v}_0 = \kappa \delta^{(2)}(\boldsymbol{\rho}) \mathbf{e}_z$, where $\delta^{(2)}$ is a two-dimensional delta function and $\boldsymbol{\rho}$ a vector in the xy-plane [25]. The rotation of a vortical system is thus not identically zero, but rather vanishes at every point where the condensate density is non-zero. It is interesting to compare the velocity in Eq. (3.13) with that of rigid rotation with angular velocity $\boldsymbol{\Omega}$, which has the velocity field $\mathbf{v} = \boldsymbol{\Omega} \times \mathbf{r}$ with the rotation $\nabla \times \mathbf{v} = 2\boldsymbol{\Omega}$ [24]. Since the rotation is necessarily non-zero everywhere it is thus impossible for a superfluid to flow rigidly.

If the dominant energy contribution of the vortex line comes from the flow energy then we can estimate the energy per unit length $\mathcal{E}_l$ for a single vortex line in a uniform condensate according to [72]

$$\mathcal{E}_1 = \frac{n_0}{2} \int \mathrm{d}\sigma \, \mathbf{v}_0 \cdot \mathbf{v}_0 \approx \pi n_0 s^2 \int_{r_c}^{R} \frac{\mathrm{d}\rho}{\rho} = \pi n_0 s^2 \ln\left(\frac{R}{r_c}\right). \qquad (3.14)$$

Here R is the radius of the condensate and r_c the radius of the vortex core, introduced in order to avoid the divergence in the lower limit of the integral[2]. For two parallel vortex lines there is an additional contribution to the energy density associated with their interaction, which can be estimated for the velocity field $\mathbf{v} = \mathbf{v}_1 + \mathbf{v}_2$ with $\mathbf{v}_1 = s_1 \mathbf{e}_\varphi / \rho$ and

$$\mathbf{v}_2 = s_2 \frac{\mathbf{e}_z \times (\mathbf{r} - \mathbf{r}_0)}{|\mathbf{e}_z \times (\mathbf{r} - \mathbf{r}_0)|^2}, \qquad (3.15)$$

where $\mathbf{r}_0 = (d, 0, 0)$ points to the center of the second vortex line. The energy density associated with the interaction is then [72]

$$\mathcal{E}_{\mathrm{int}} = n_0 s_1 s_2 \int \mathrm{d}\sigma \frac{\rho - d\cos\varphi}{\rho(\rho^2 - 2\rho d\cos\varphi + d^2)} \approx 2\pi n_0 s_1 s_2 \ln\left(\frac{R}{d}\right), \qquad (3.16)$$

where it has been assumed that $r_c \ll d \ll R$. The total energy density for two vortex lines is thus

$$\mathcal{E}_2 = \pi n_0 (s_1 + s_2)^2 \ln\left(\frac{R}{r_c}\right) - 2\pi n_0 s_1 s_2 \ln\left(\frac{d}{r_c}\right), \qquad (3.17)$$

showing that for a given amount of circulation in a uniform system it is energetically favorable to have multiple singly-quantized vortices over multiply-quantized ones. Although similar results are found for weakly-interacting condensates in harmonic confinements [73, 74], this is not necessarily the case in general, and multiply-quantized vortices have been shown to be stable in for example anharmonic trapping potentials [75, 76]. An example of vortex ground states of a one-component condensate with short-range interactions in an azimuthally symmetric harmonic trap

---

[2]This divergence comes from the assumption of an everywhere uniform condensate, and as long as the density around the vortex core goes to zero as $n_0 \sim \rho$ or faster when $\rho \to 0$ there is no divergence.

$\Omega = 0.00$ $\Omega = 0.40$ $\Omega = 0.50$

$\Omega = 0.55$ $\Omega = 0.60$ $\Omega = 0.66$
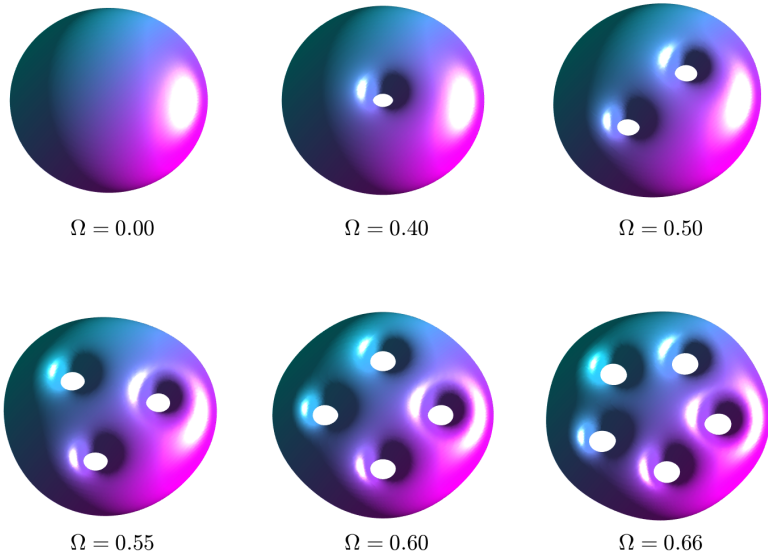
Figure 3.1: Ground-state density isosurfaces for a one-component condensate with short-range interactions in a rotating harmonic trap with rotation frequencies as indicated by the figure. The data has been obtained numerically by propagating Eq. (2.30) in imaginary time in the frame rotating with the trap for the dimensionless parameters $N = 10000$, $g = 0.05$, $\varepsilon_{dd} = 0$, $\omega = 1$, and $\lambda = 2$ for the trap in Eq. (3.18). The density isosurfaces are taken at $|\Phi|^2 = 70$.

$$V_{ext}(\mathbf{r}) = \frac{\omega^2}{2}(\rho^2 + \lambda^2 z^2) \tag{3.18}$$

which is set to rotate is shown in Fig. 3.1. The figure shows how the number of vortices grows one by one as the rotation frequency is increased. When this number becomes large enough the vortices eventually form an ordered triangular lattice structure [77, 78], see Fig. 3.2 for an example. In Paper I we investigate the existence of self-bound droplets containing multiple singly-quantized vortices in two-dimensional binary Bose mixtures and in Paper III we study the breathing mode of vortical droplets—also in two-dimensional mixtures.
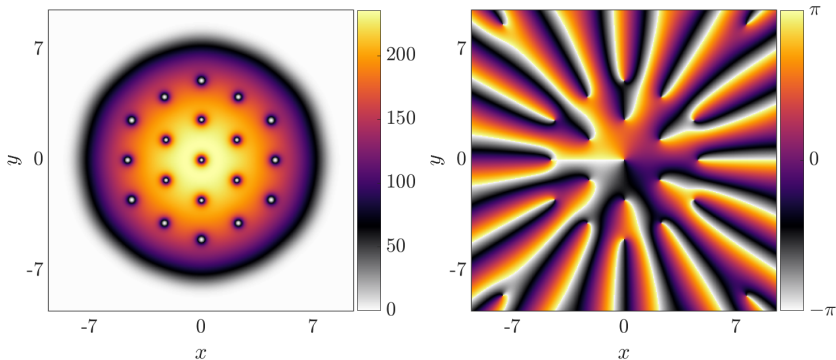
**Figure 3.2:** Ground-state density *(left)* and phase *(right)* in the xy-plane at $z = 0$ for a one-component condensate with short-range interactions in a rotating harmonic trap. The data has been obtained numerically by propagating Eq. (2.30) in imaginary time in the frame rotating with the trap for the dimensionless parameters $N = 100000$, $g = 0.1$, $\varepsilon_{dd} = 0$, $\omega = 1$, $\lambda = 2$, and $\Omega = 0.58$ for the trap in Eq. (3.18).

3.3 Metastable Superflow

Another interesting effect that has been observed in superfluids is the ability to remain in a state with nonzero angular momentum for a long time[3] even when the external trapping potential does not rotate [67, 68]. Such a spinning state can not be the ground state, but instead corresponds to some metastable configuration. To understand this phenomenon we consider a fluid in a cylindrically symmetric trap rotating around the symmetry axis with angular frequency Ω. The energy in the frame rotating with the trap is $E(L) = E_0(L) - \Omega L$, where E_0 is the energy in the laboratory frame and L the angular momentum. For a fluid rotating rigidly the rotational energy is $L^2/(2I_{\text{rig}})$ and the total energy is consequently minimized for $L = \Omega I_{\text{rig}}$. For a superfluid the situation is different since the circulation is quantized and the velocity field can not take the rigid form $\rho \Omega \mathbf{e}_\varphi$. To illustrate how metastable flow in a superfluid can come about we again consider the one-component condensate with short-range interactions in a rotating trap. Figure 3.3 shows the ground-state energy $E_0(L)$ as a function of the angular momentum L, computed numerically from Eq. (2.30) under the constraint that the angular momentum is fixed [81]. When the trap is purely harmonic the energy is a

---

[3]For example, a long time is about 10 s for the experiment in Ref. [79] and 40 s for the experiment in Ref. [80].
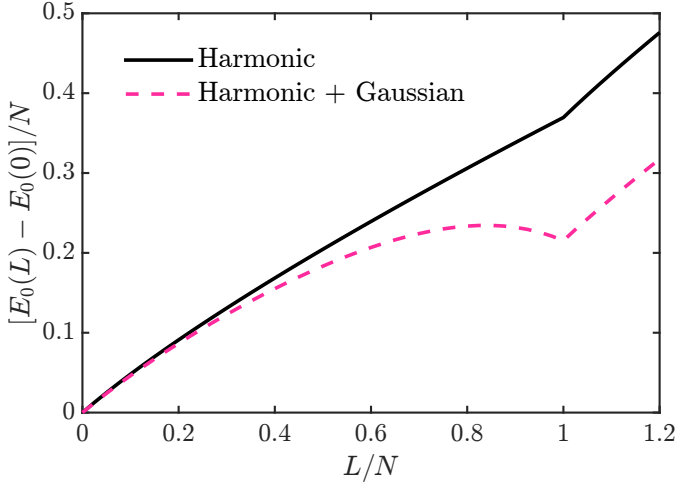
Figure 3.3: Ground-state energy in the laboratory frame as a function of angular momentum for a one-component condensate with short-range interactions in *(a)* the purely harmonic trap in Eq. (3.18) *(solid black line)* and *(b)* the harmonic trap with a repulsive Gaussian in Eq. (3.19) *(dashed pink line)*. The data has been obtained numerically by propagating Eq. (2.30) in imaginary time for the dimensionless parameters $N = 10000$, $g = 0.05$, $\varepsilon_{dd} = 0$, $\omega = 1$, $\lambda = 2$, $V_0 = 5$ and $w = 2$ under the constraint that the angular momentum is fixed.

monotonically increasing function with a kink at $L/N = 1$. In the rotating frame where the energy is lowered by $-\Omega L$ this kink can become the global energy minimum above some critical Ω such that the number of vortices in the ground state changes from zero to one. If the rotation is stopped the $L = 0$ state becomes the lowest in energy once more and the system reverts back to the non-rotating configuration[4], and there can consequently be no metastable flow for the harmonic case. This situation can change by adding an external repulsive potential to the center of the trap, and it can be seen in Fig. 3.3 that for a trap of the form

$$V_{\text{ext}}(\mathbf{r}) = \frac{\omega^2}{2}(\rho^2 + \lambda^2 z^2) + V_0 e^{-2\rho^2/w^2}, \tag{3.19}$$

the energy exhibits a local minimum at $L/N = 1$, corresponding to a metastable one-vortex state which is protected against decay by an energy barrier consisting

---

[4]Strictly speaking for cylindrically symmetric traps such as the ones in Eq. (3.18) or Eq. (3.19) angular momentum is conserved and there should consequently be no changes between states. If such conservation laws are relaxed just slightly, however, the reasoning holds.
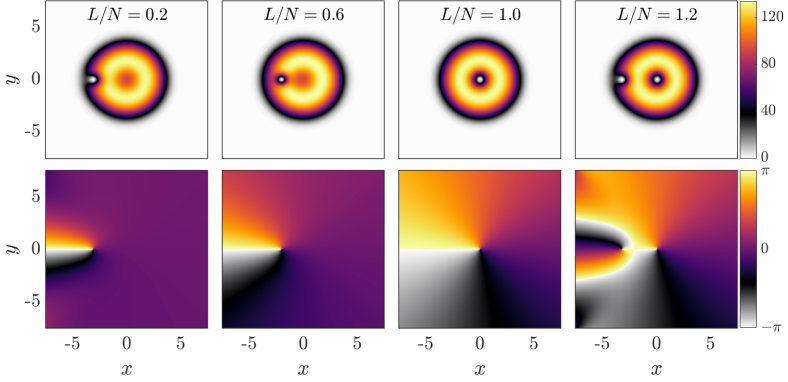
Figure 3.4: Ground-state densities *(top row)* and the corresponding phases *(bottom row)* in the xy-plane at $z = 0$ for a one-component condensate with short-range interactions in a harmonic trap with a repulsive Gaussian for different values of the angular momentum as indicated by the figure. The data has been obtained numerically by propagating Eq. (2.30) in imaginary time for the dimensionless parameters $N = 10000$, $g = 0.05$, $\varepsilon_{dd} = 0$, $\omega = 1$, $\lambda = 2$, $V_0 = 5$, and $w = 2$ for the trap in Eq. (3.19) under the constraint that the angular momentum is fixed.

of off-center vortex states, see Fig. 3.4. In Paper I we use the idea of metastable superflow as a potential way to generate droplets containing vorticity, and in Paper II and Paper IV we study the existence of such metastable flow in dipolar supersolids and in droplet-superfluid compounds made out of binary Bose mixtures with short-range interactions, respectively.

Chapter 4

Supersolidity

The supersolid state of matter has to date been experimentally realized in three different types of atomic gases: by coupling a condensate to the modes of optical cavities [13]; by using spin-orbit coupling [14]; or by using atoms with a strong dipole moment [15–17]. This chapter introduces the idea of what it means to be a supersolid, with a focus on the dipolar variety.

4.1 Defining Supersolidity

The 'super' in supersolidity comes, of course, from superfluidity[1], and refers to a state of matter which in some sense is both superfluid *and* solid [8–12]. A solid can be defined by considering the deviation of the density from the average $\delta n(\mathbf{r}) \equiv \bar{n} - n(\mathbf{r})$, where $n(\mathbf{r})$ is the density and

$$\bar{n} = \frac{1}{V} \int d\mathbf{r}\, n(\mathbf{r}) \tag{4.1}$$

is the averaged density in some volume V. We define a crystalline solid[2] as having

---

[1] The 'super' in superfluidity, on the other hand, was introduced in analogy with superconductivity.

[2] There can also be other types of solids such as glasses which possess structure but in a disordered manner.

a non-vanishing deviation satisfying

$$\delta n(\mathbf{r}) = \delta n(\mathbf{r} + \mathbf{T}_i) \qquad (4.2)$$

for some discrete set of lattice vectors $\{\mathbf{T}_i\}$ [82]. This property is referred to as (diagonal) long-range order and warrants some discussion. First of all it is assumed to be an intrinsic property such that the translational symmetry is broken spontaneously, as opposed to being induced by an external structure such as, for example, an optical lattice. Conversely, one can imagine modifying the density externally such that the condition in Eq. (4.2) does not hold for an actual solid. The definition of a solid from the existence of long-range order as expressed by Eq. (4.2) is thus not immediately applicable to a general system and has to be considered in some limit where the external influence goes to zero. Even so, this definition can nevertheless help us gain some intuition as to what we mean by a solid. Having established what a constitutes a solid, a supersolid can then be defined as a solid that also exhibits signatures of superfluidity.

4.2   Non-Classical Rotational Inertia

In the search for a useful quantity to characterize the degree of superfluidity of a supersolid we are guided by the experimental result that the angular momentum of superfluids in cylindrically symmetric traps remains at zero when the external potential is set to rotate slowly around the symmetry axis [66]. This motivates the definition of the fraction of non-classical rotational inertia f as [83]

$$f \equiv 1 - \frac{I}{I_{\mathrm{rig}}}, \qquad (4.3)$$

where $I \equiv \lim_{\Omega \to 0} L/\Omega$ is the total rotational inertia, Ω the rotation frequency, L the expectation value of the z-component angular momentum operator, and $I_{\mathrm{rig}} = \int \mathrm{d}\mathbf{r}\, n(\mathbf{r})\rho^2$ the rotational inertia for rigid rotation. In Ref. [83], which studies a collection of particles in an annulus with a radius much larger than its thickness, the quantity in Eq. (4.3) is used to define the superfluid density according to $n_s \equiv nf$. An upper bound for f is subsequently derived which is equal to [83]

$$f^+ = (2\pi)^2 \left[\int_0^{2\pi} \mathrm{d}\varphi\, n_{xs}(\varphi) \int_0^{2\pi} \frac{\mathrm{d}\varphi}{n_{xs}(\varphi)} \right]^{-1}, \qquad (4.4)$$

where φ is the azimuthal angle and n_{xs} the density averaged over the cross section of the annulus. From the Cauchy-Schwarz inequality it follows that $f^+ \leq 1$, with equality occurring when n_{xs} is constant. The introduction of a density modulation consequently decreases this upper bound from unity such that the superfluid density can not make up the whole system, even at zero temperature. If there exist regions where n_{xs} is small such that $\int_0^{2\pi} \mathrm{d}\varphi/n_{xs}(\varphi) \gg 1$ then $f^+ \to 0$, corresponding to a separation of localized parts whose motion according to Eq. (4.3) must be rigid.

4.3 The Dipolar Supersolid

4.3.1 The Roton Mode

The transition to a spontaneously density-modulated state in dipolar condensates can be understood by analyzing the excitation spectrum which, depending on the parameters of the system, may develop a rotonic character [84–86]. The hallmark of the rotonic spectrum is that the excitation energy has a minimum at some finite momentum, the existence of which we can understand by imagining a condensate in a tubular trap along a direction orthogonal to the polarization direction of the dipoles. Let the confinement length in the polarization direction be l and consider excitations along the tube with momentum k, corresponding to density modulations with wavelength $2\pi/k$. For long wavelength excitations such that $kl \ll 1$ the side-by-side repulsion of the dipole-dipole interaction dominates, resulting in an increase in the excitation energy with increasing k. Increasing the momentum to values $kl \sim 1$ leads to excitations where the attractive head-to-tail configurations participate, which can decrease the energy. For even higher momenta eventually the kinetic energy starts to dominate and the energy increases again, resulting in a minimum in the dispersion relation. If the parameters of the dipolar system are tuned such that the energy gap of the roton minimum disappears we find that the ground state develops a periodically modulated structure with spontaneously broken translational symmetry [38, 87, 88]. Much like self-bound dipolar droplets without external trapping these configurations are expected to be unstable

at a mean-field level [89], but emerge in a beyond mean-field formalism where the increased repulsion from quantum fluctuations serves to stabilize the system [21, 22, 30, 37, 38].

4.3.2   All Things Rings

The alleged superfluidness of the supersolid invites a study of its rotational properties, and we consider to this end a dipolar condensate at zero temperature goverened by Eq. (2.30) in a ring-shaped trap

$$V_{\text{ext}}(\mathbf{r}) = \frac{\omega^2}{2} \left[(\rho - \rho_0)^2 + \lambda^2 z^2 \right], \tag{4.5}$$

where ρ_0 is the radius of the ring. The discussions and results in this section are similar to much of what is presented in Paper II and Paper IV. In order to characterize the phases of the system we investigate the fraction of non-classical rotational inertia f as defined in Eq. (4.3). For a pure superfluid $f = 1$ and for rigid-body motion $f = 0$, and a supersolid is therefore expected to have values somewhere in between.
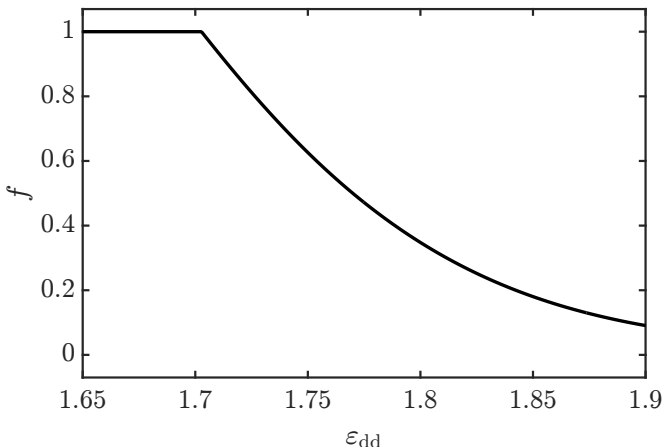
Figure 4.1: The fraction of non-classical rotational inertia f as a function of the relative interaction strength ε_{dd} for a dipolar one-component condensate in a ring trap. The data has been obtained numerically by propagating Eq. (2.30) in imaginary time in the frame rotating with the trap for the dimensionless parameters $N = 18000$, $g_{\text{dd}} = 0.15$, $\omega = 2.5$, $\lambda = 1.5$, $\rho_0 = 3$, and $\Omega = 0.0001$ for the trap in Eq. (4.5).
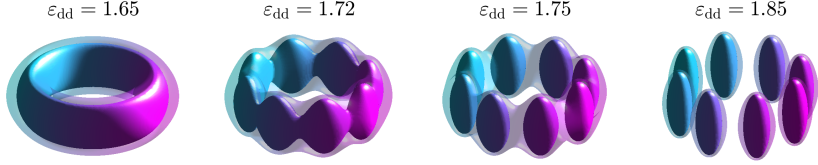
Figure 4.2: Ground-state density isosurfaces for a dipolar one-component condensate in a ring trap for different values of the relative interaction strength $\varepsilon_{\mathrm{dd}}$ as indicated by the figure. The data has been obtained numerically by propagating Eq. (2.30) in imaginary time for the dimensionless parameters $N = 18000$, $g_{\mathrm{dd}} = 0.15$, $\omega = 2.5$, $\lambda = 1.5$, and $\rho_0 = 3$ for the trap in Eq. (4.5). The isosurfaces are taken at $|\Phi|^2 = 100$ for the solid surface and at $|\Phi|^2 = 20$ for the transparent one.

Figure 4.1 shows the numerically computed f as a function of the relative interaction strength $\varepsilon_{\mathrm{dd}}$, where it is displayed how the fraction of non-classical rotational inertia takes on values $0 < f < 1$ above some critical $\varepsilon_{\mathrm{dd}} \approx 1.7$. The decrease of f from unity marks the onset of a modulation of the condensate density along the ring, see Fig. 4.2. For this particular system there are eight lattice sites, and associated with each site is a macroscopic amount of particles taking the form of a droplet. These droplets are connected to each other by a low-density part of the condensate, a link that becomes weaker and weaker as f is decreased until left is but a collection of droplets with negligible density overlap.

The question regarding the existence of metastable superflow in the ring-shaped supersolid can be addressed by calculating the energy in the laboratory frame $E_0(L)$ as a function of the angular momentum L, see the numerical results in Fig. 4.3. In the superfluid phase for $\varepsilon_{\mathrm{dd}} = 1.65$ the energy has for the most part a negative curvature with minima at integer values of L/N, representing the entry of vortices into the condensate from the outside as discussed in the previous chapter. Around integer values of L/N for $\varepsilon_{\mathrm{dd}}$ close to the supersolid phase we find that $E_0(L)$ is roughly linear, where the corresponding condensate density has acquired a density modulation along the ring, even though the condensate at $L = 0$ is superfluid. Such supersolid "shortcuts" are investigated in Paper II, where it is found that the different rotational behavior of the supersolid can be energetically favorable compared to the vortex entry in the superfluid close to the phase transition. The energy in the supersolid phase has a positive curvature with a functional behavior that appears to be intersecting parabolae. This can be explained by imagining the system to be able to take angular momentum in two ways: through quantized vorticity and through rigid rotation. For simplicity we consider in the following
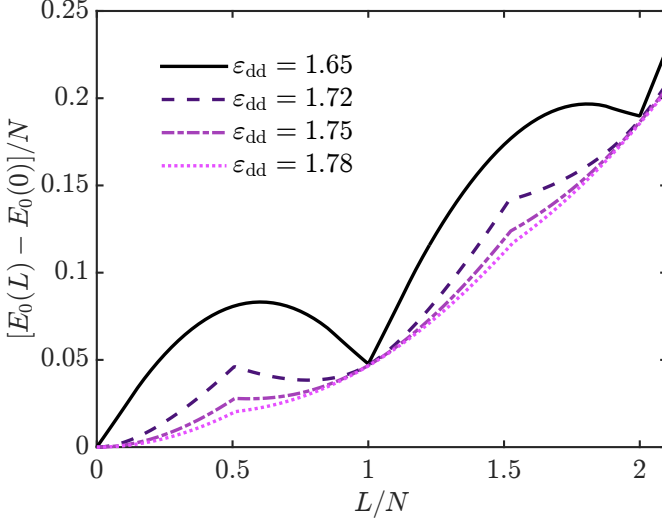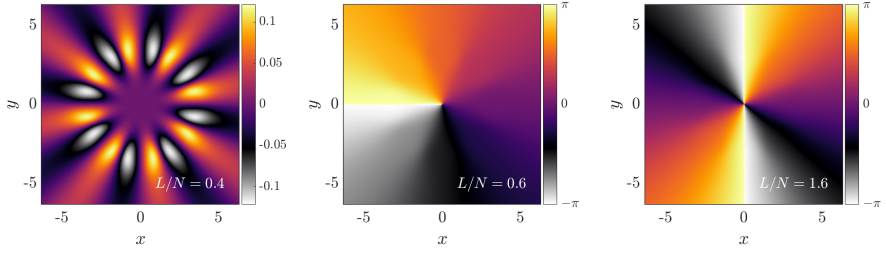
Figure 4.3: Ground-state energy as a function of angular momentum in the laboratory frame for a dipolar one-component condensate in a ring trap at different values of ε_{dd} as indicated by the legend. The data has been obtained numerically by propagating Eq. (2.30) in imaginary time for the dimensionless parameters $N = 18000$, $g_{dd} = 0.15$, $\omega = 2.5$, $\lambda = 1.5$, and $\rho_0 = 3$ for the trap in Eq. (4.5) under the constraint that the angular momentum is fixed.

a "thin" ring $\rho_0 \gg 1/\sqrt{\omega}$ such that the condensate can be approximated to be non-negligible only for values $\rho \approx \rho_0$. We first estimate the energy cost of adding an s-times multiply quantized vortex to an azimuthally symmetric ring-shaped superfluid under this assumption. If the dominant energy contribution is the flow energy, then for the azimuthal flow in Eq. (3.13) the energy cost per particle for the thin ring is simply $s^2/(2\rho_0^2)$. Now, assuming that a fraction f_v of the total particles of the supersolid host an s-times quantized vortex and the rest of the particles rotate rigidly, this leads to the rotational energy

$$E_s(L)/N = \frac{1}{2\rho_0^2} \left[\frac{(L/N - f_v s)^2}{(1 - f_v)} + f_v s^2 \right]. \tag{4.6}$$

These parabolic energy branches satisfy $E_{s+1} = E_s$ for $L/N = s + 1/2$, i.e. the ground state should according to this model have no vortex for $L/N < 1/2$, a single vortex for $1/2 < L/N < 3/2$ and so on. This is in good agreement with the numerical data shown in Fig. 4.3 where the parabolae intersect at approximately half-integer values of L/N, and it can be confirmed that these intersections correspond to the proper change in s by studying the phase of the order parameter,

Figure 4.4: Ground-state phases in the xy-plane at $z = 0$ for a dipolar one-component condensate in a ring trap at different values of the angular momentum as indicated by the figure. The data has been obtained numerically by propagating Eq. (2.30) in imaginary time for the dimensionless parameters $N = 18000$, $g_{dd} = 0.15$, $\varepsilon_{dd} = 1.75$, $\omega = 2.5$, $\lambda = 1.5$, and $\rho_0 = 3$ for the trap in Eq. (4.5) under the constraint that the angular momentum is fixed.

see Fig. 4.4 for an example when $\varepsilon_{dd} = 1.75$. With this interpretation it is immediate to see when there can exist local minima in the energy $E_0(L)$, since the minimum of $E_s(L)$ occurs at $L/N = f_v s$. This minimum exists in the total energy only if $E_s(L)$ is the lowest energy branch for this minimizing value of L/N, which is true for $s - 1/2 < L/N < s + 1/2$, and the existence condition for a minimum corresponding to an s-times quantized vortex thus reads $f_v > (s - 1/2)/s$. The decay of such a vortex state is in this case protected by an energy barrier where there is rigid rotation in the direction opposite to that of the vortex, allowing for the existence of metastable superflow in the supersolid. Although the fraction of non-classical rotational inertia f and the vortex fraction f_v are defined differently, they might be surmised to be equal since they are both tied to the degree of superfluidity of the system. The aforementioned model provides a simple way to test this hypothesis, since the local minimum in $E_0(L)$ corresponding to an $s = 1$ vortex should occur exactly at $L/N = f_v$ whenever $f_v > 1/2$. From Figs. 4.1 and 4.3 it can be seen that the location of this minimum occurs for values a bit lower than the corresponding f, for example for $\varepsilon_{dd} = 1.72$ the non-classical rotational inertia fraction is $f \approx 0.85$ and the first minimum occurs at $L/N \approx 0.78$, while for $\varepsilon_{dd} = 1.75$ we have $f \approx 0.63$ with a minimum at $L/N \approx 0.55$. Despite this discrepancy, the qualitative behavior of the two quantities are in agreement, i.e. the first local minimum moves to smaller values of L/N as f decreases. It should be noted that the difference in f and f_v could be explained by the fact that in the model we assumed a thin ring $\rho_0 \gg 1/\sqrt{\omega}$, whereas for the numerical data $\rho_0 = 3$ and $1/\sqrt{\omega} \approx 0.63$. Furthermore, the density and rotational inertia of the system may change as angular momentum is added to it, and would then not be the same

as in the definition of f which is taken in the limit $\Omega \to 0$.

Some insights regarding the flow patterns in the supersolid can be obtained by considering a condensate in a rotating quasi one-dimensional ring where the azimuthal angle φ is the only relevant coordinate. It should be emphasized that the dipolar supersolid discussed here is a three-dimensional entity, however studying the dimensionally reduced system may nevertheless shed some light on the flow behavior. By substituting $\Phi(\varphi) = \sqrt{n_0(\varphi)}e^{i\phi(\varphi)}$ into Eq. (2.30) for the rotating frame and identifying real and imaginary parts we obtain two equations, where the equation for the imaginary part is

$$\sqrt{n_0}\frac{\partial v_\varphi}{\partial \varphi} + 2\frac{\partial \sqrt{n_0}}{\partial \varphi}v_\varphi = 2\rho_0\Omega\frac{\partial \sqrt{n_0}}{\partial \varphi}, \qquad (4.7)$$

which has the velocity solution $v_\varphi(\varphi) = \rho_0\Omega + C/n_0(\varphi)$, where C is an integration constant. This constant can be expressed in terms of the circulation in Eq. (3.12), giving the velocity

$$v_\varphi(\varphi) = \rho_0\Omega + \frac{\kappa - \kappa_{\text{rig}}}{\rho_0\Lambda n_0(\varphi)}, \qquad (4.8)$$

where $\kappa_{\text{rig}} \equiv 2\pi\rho_0^2\Omega$ is the circulation for rigid rotation and $\Lambda \equiv \int_0^{2\pi} \mathrm{d}\varphi/n_0(\varphi) > 0$. Consider now the case where $\kappa = 0$, which is expected for sufficiently low rotation frequencies since the circulation is quantized. The second term in Eq. (4.8) is then negative, and vanishes in regions where the density is large $n_0 \gg 2\pi/\Lambda$ such that the motion is approximately rigid $v_\varphi \approx \rho_0\Omega$. As the density decreases so does the velocity, and when $n_0 < 2\pi/\Lambda$ the velocity switches sign $v_\varphi < 0$, i.e. regions with sufficiently low density flow in the opposite direction to that of the high-density regions. This behavior is exemplified in the leftmost panel in Fig. 4.4, where the periodic behavior of the phase around the ring indicates a repeated change in the velocity direction. Interestingly, if we assume that the droplet crystals of the supersolid move approximately rigidly, then because of the counterflow of the low-density regions the fraction $1 - f$ is lower than the fraction of particles associated with the crystals. If we further assume that $f = f_v$, then the vortex fraction must be higher than that of the low-density residual condensate, i.e. also the crystalline structure has to be involved in the formation of vortices.
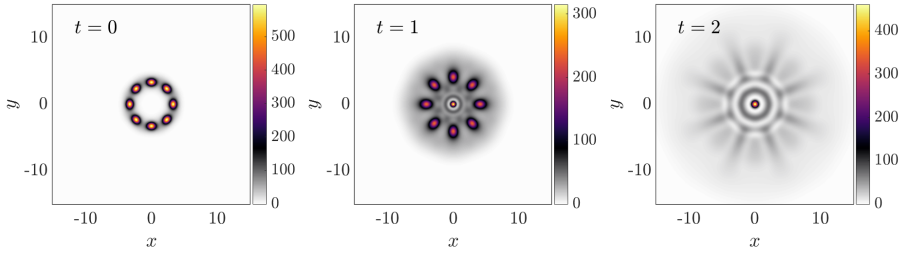
Figure 4.5: Time evolution of the ground-state density for a dipolar one-component condensate in a ring trap as the radial trap is turned off at $t = 0$, shown for the xy-plane at $z = 0$. The data has been obtained numerically by first propagating Eq. (2.30) in imaginary time in order to obtain the ground state, which is then propagated in real time using the same equation. The dimensionless parameters are $N = 18000$, $g_{dd} = 0.15$, $\varepsilon_{dd} = 1.75$, $\omega = 2.5$, $\lambda = 1.5$ and $\rho_0 = 3$ for the trap in Eq. (4.5).

We now consider what happens to the toroidal supersolid when the radial trap is turned off and the system is allowed to expand. Figure 4.5 shows the expansion of a configuration which initially has no angular momentum, and it can be seen how the droplets expand from the center due to the long-range side-by-side repulsion of the dipole-dipole interaction while decreasing in density, which has been observed also for a release from a harmonic trap [90]. Interestingly, a high-density region forms at the center as a result of the interference of the dispersing condensate. If we instead imagine rotating the same system until it acquires one vortex, then stop rotating it such that it ends up in an energy minimum corresponding to a persistent current, and then finally turn off the radial trap, we find a situation as shown in Fig. 4.6. The addition of angular momentum to the initial configuration results in a swirling of the low-density regions, and the formation of a high-density region at the center is now prohibited by the existence of a vortex core there.

The ring-shaped supersolids that have been investigated in this section are particularly simple systems for studying rotational behavior since the density at the position where a vortex core appears is low in the abscence of vorticity. When this is not the case, as in for example a harmonic trap, vortex formation is energetically favorable in the low-density regions of the supersolid, which may compete against the vortices' inclination to arrange themselves in a triangular lattice structure [90]. Interestingly, for dipolar supersolids in harmonic traps [37, 90], with periodic boundary conditions in the plane [91, 92], or in box potentials [93], the optimal ordering of the high-density droplets is also that of a triangular lattice.
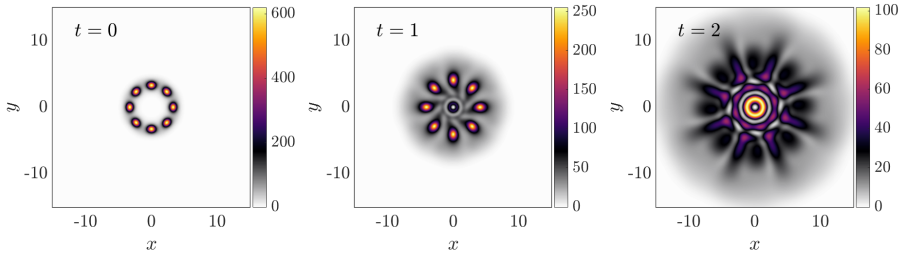
Figure 4.6: Time evolution of the ground-state density for a dipolar one-component condensate in a ring trap with $L/N = 0.55$ as the radial trap is turned off at $t = 0$, shown for the xy-plane at $z = 0$. The data has been obtained numerically by first propagating Eq. (2.30) in imaginary time under the constraint that the angular momentum is fixed in order to obtain the ground state, which is then propagated in real time using the same equation. The dimensionless parameters are $N = 18000$, $g_{dd} = 0.15$, $\varepsilon_{dd} = 1.75$, $\omega = 2.5$, $\lambda = 1.5$ and $\rho_0 = 3$ for the trap in Eq. (4.5).

4.4 A One-Droplet "Supersolid"

Let us end this chapter by briefly discussing an interesting situation that can occur in Bose-Bose mixtures with short-range interactions. If the binary system is in a self-bound droplet state and we try to add more particles to one of the components these will not be able to bind to the droplet and instead disperse [23]. By capturing this surplus of particles with an external trapping potential it is possible to obtain a structure where a droplet coexists with a residual superfluid, see Fig. 4.7 for an example in a ring trap. If we define the non-classical rotational inertia fraction of each component according to

$$f_\sigma \equiv 1 - \frac{I_\sigma}{I_{\text{rig}}}, \tag{4.9}$$

where I_σ is the rotational inertia of component σ, then the component with the surplus of particles can exhibit non-classical rotational inertia where the fraction is smaller than unity (for the numerical data in Fig. 4.7 the fraction of the second component is $f_2 \approx 0.85$). Figure 4.7 shows the existence of a single droplet crystal which is connected to itself through a link of superfluid. Such a configuration can obviously not be called a supersolid according to the definition of crystalline long-range order in Eq. (4.2) since there is only one "lattice site", and splitting this droplet into multiple ones would come at a cost in kinetic energy without any gain. Regardless, this type of system exhibits spontaneous localization as a result
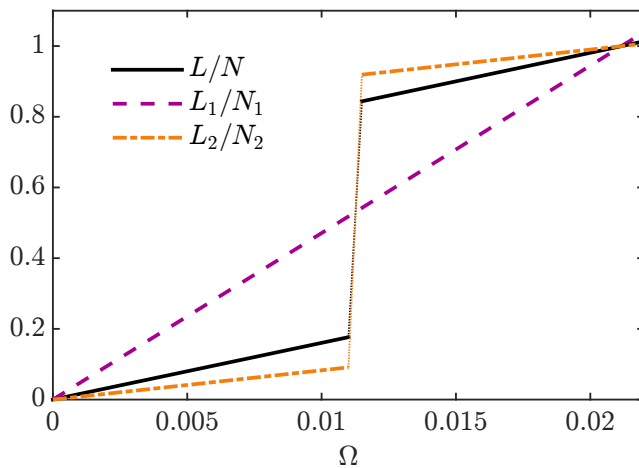
44
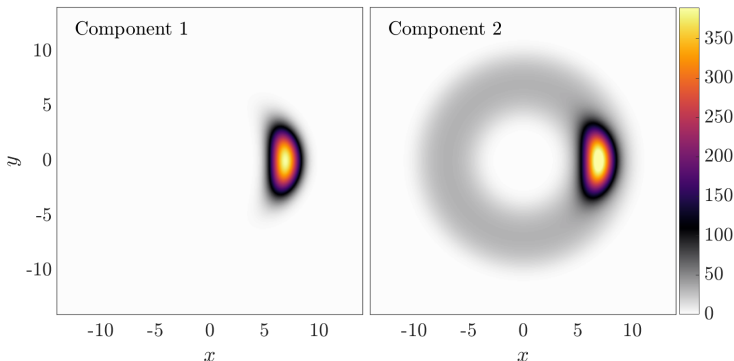
Figure 4.7: Ground-state densities in the xy-plane at $z = 0$ for a two-component condensate with short-range interactions in a ring trap. The data has been obtained numerically by propagating Eq. (2.45) in imaginary time in the frame rotating with the trap for the dimensionless parameters $N_1 = 10000$, $N_2 = 40000$, $g_{11} = g_{22} = 0.05$, $g_{12} = -0.055$, $\omega = 0.5$, $\lambda = 1$, and $\rho_0 = 7$ for the trap in Eq. (4.5).

of the interactions between the particles, as well as simultaneous rigid and superfluid behavior under rotation. The latter property is exemplified in Fig. 4.8, which shows the angular momentum per particle of each component and the total angular momentum per particle as a function of the rotation frequency. It can be seen how the component with extra particles ($\sigma = 2$ in this example) displays both the linear slopes associated with rigid motion, as well as a discontinuous jump in angular momentum connected to quantized vorticity. The critical rotation frequency Ω_{crit}, above which an s-times quantized vortex becomes energetically favorable, can be estimated in the model of the previous section by using the energies in Eq. (4.6), yielding

$$\Omega_{\text{crit}} = \frac{2s - 1}{2\rho_0^2}. \tag{4.10}$$

This in fairly good agreement with the numerical results presented in Fig. 4.8, where $\Omega_{\text{crit}} \approx 0.010$ for the analytical model versus $\Omega_{\text{crit}} \approx 0.011$ for the numerical results. In Paper IV we study a compound system similar to the one presented in this section, but instead in one dimension with periodic boundary conditions. We find there that the energy as a function of angular momentum for the droplet-superfluid compound is similar to that of a dipolar supersolid, and that there exists an extra gapless mode in this phase compared to the uniform one.

Figure 4.8: The total angular momentum per particle and the angular momentum per particle in each component as a function of the rotation frequency of the ground state for a two-component condensate with short-range interactions in a ring trap. The data has been obtained numerically by propagating Eq. (2.45) in imaginary time in the frame rotating with the trap for the dimensionless parameters $N_1 = 10000$, $N_2 = 40000$, $g_{11} = g_{22} = 0.05$, $g_{12} = -0.055$, $\omega = 0.5$, $\lambda = 1$, and $\rho_0 = 7$ for the trap in Eq. (4.5).

Chapter 5

Outlook

In this thesis we have investigated superfluid and supersolid properties of cold atomic gases beyond mean field. Although the extended Gross-Pitaevskii formalism employed throughout this thesis often succeeds in achieving qualitative correctness, it has been shown to fail in its accuracy in some places. For example, it has been demonstrated that the predicted critical number of particles required to form self-bound droplets in three dimensions differs from experiments for both dipolar condensates [94] and mixtures [35]. Additionally, it has been found that theoretical results including beyond mean-field effects for the roton mode agree worse with experiments than a pure mean-field description [95].

With these demonstrated disagreements between theory and experiments in mind, it is interesting to address some of the limitations of the extended mean-field formalism. First of all, as outlined in chapter 2, quantum fluctuations are incorporated in a quasi-homogeneous and quasi-static way, and any considerable spatial or temporal variations should therefore diminish the accuracy of the description. Furthermore, the perturbative nature of the formalism restricts the parameter regime: to low densities and weak interactions in three dimensions [21–23]; to weak interactions in two dimensions [61]; and to weak interactions and high densities in one dimension [61]. Another question concerns the Bogoliubov modes of the system, which in the droplet parameter regime can turn imaginary [21–23, 61]. This imaginary part is neglected in the extended Gross-Pitaevskii equation, and one

might question the legitimacy of such an omission[1]. Alternative proposals that do not rely on ignoring these imaginary modes have been suggested, for example by incorporating higher-order terms [96] or by introducing bosonic pairing [97, 98].

Finally, we conclude this thesis with some interesting open questions. Can a supersolid flow through a thin capillary frictionlessly? How does the interplay of quantum and thermal fluctuations affect the supersolid and the associated breaking of symmetries? How do the Bogoliubov and exact spectra of excitations compare for droplets or supersolids? To what extent are droplet-superfluid mixtures in binary systems with short-range interactions similar to dipolar supersolids? Will these exotic states of matter ever have any practical use? All of these questions and more hint towards an exciting future for the field of ultracold atomic gases, bounded perhaps only by curiosity.

---

[1]Although the neglect of such an imaginary part is not necessary for the existence of one-dimensional droplets in mixtures.

References

[1] S. N. Bose, Z. Phys. **26**, 178 (1924).

[2] A. Einstein, Sitzber. Preuss. Akad. Wiss. (Berlin) **22**, 261 (1924).

[3] M. H. Anderson, J. R. Ensher, M. R. Matthews, C. E. Wieman, and E. A. Cornell, Science **269**, 198 (1995).

[4] K. B. Davis, M. O. Mewes, M. R. Andrews, N. J. van Druten, D. S. Durfee, D. M. Kurn, and W. Ketterle, Phys. Rev. Lett. **75**, 3969 (1995).

[5] C. C. Bradley, C. A. Sackett, J. J. Tollett, and R. G. Hulet, Phys. Rev. Lett. **75**, 1687 (1995).

[6] P. Kapitza, Nature **141**, 74 (1938).

[7] J. F. Allen and A. D. Misener, Nature **141**, 75 (1938).

[8] E. P. Gross, Phys. Rev. **106**, 161 (1957).

[9] C. N. Yang, Rev. Mod. Phys. **34**, 694 (1962).

[10] A. F. Andreev and I. Lifshitz, Zh. Eksp. Teor. Fiz. **56**, 2057 (1969).

[11] G. V. Chester, Phys. Rev. A **2**, 256 (1970).

[12] A. J. Leggett, Phys. Rev. Lett. **25**, 1543 (1970).

[13] J. Léonard, A. Morales, P. Zupancic, T. Esslinger, and T. Donner, Nature **543**, 87 (2017).

[14] J.-R. Li, J. Lee, W. Huang, B. Burchesky, F. C. Top, A. O. Jamison, and W. Ketterle, Nature **543**, 91 (2017).

[15] F. Böttcher, J.-N. Schmidt, M. Wenzel, J. Hertkorn, M. Guo, T. Langen, and T. Pfau, Phys. Rev. X **9**, 011051 (2019).

[16] L. Tanzi, E. Lucioni, F. Famà, J. Catani, A. Fioretti, C. Gabbanini, R. N. Bisset, L. Santos, and G. Modugno, Phys. Rev. Lett. **122**, 130405 (2019).

[17] L. Chomaz, D. Petter, P. Ilzhöfer, G. Natale, A. Trautmann, C. Politi, G. Durastante, R. M. W. van Bijnen, A. Patscheider, M. Sohmen, M. J. Mark, and F. Ferlaino, Phys. Rev. X **9**, 021012 (2019).

[18] T. D. Lee and C. N. Yang, Phys. Rev. **105**, 1119 (1957).

[19] T. D. Lee, K. Huang, and C. N. Yang, Phys. Rev. **106**, 1135 (1957).

[20] D. M. Larsen, Ann. Phys. (Berlin) **24**, 89 (1963).

[21] A. R. P. Lima and A. Pelster, Phys. Rev. A **84**, 041604 (2011).

[22] A. R. P. Lima and A. Pelster, Phys. Rev. A **86**, 063609 (2012).

[23] D. S. Petrov, Phys. Rev. Lett. **115**, 155302 (2015).

[24] L. Pitaevskii and S. Stringari, *Bose-Einstein Condensation and Superfluidity* (Oxford University Press, 2016).

[25] C. J. Pethick and H. Smith, *Bose-Einstein Condensation in Dilute Gases*, 2nd ed. (Cambridge University Press, 2008).

[26] I. Ferrier-Barbut, H. Kadau, M. Schmitt, M. Wenzel, and T. Pfau, Phys. Rev. Lett. **116**, 215301 (2016).

[27] I. Ferrier-Barbut, M. Schmitt, M. Wenzel, H. Kadau, and T. Pfau, J. Phys. B: At. Mol. Opt. Phys. **49**, 214004 (2016).

[28] L. Chomaz, S. Baier, D. Petter, M. J. Mark, F. Wächtler, L. Santos, and F. Ferlaino, Phys. Rev. X **6**, 041039 (2016).

[29] M. Schmitt, M. Wenzel, F. Böttcher, I. Ferrier-Barbut, and T. Pfau, Nature **539**, 259 (2016).

[30] F. Wächtler and L. Santos, Phys. Rev. A **93**, 061603 (2016).

[31] R. N. Bisset, R. M. Wilson, D. Baillie, and P. B. Blakie, Phys. Rev. A **94**, 033619 (2016).

[32] D. Baillie, R. M. Wilson, R. N. Bisset, and P. B. Blakie, Phys. Rev. A **94**, 021602 (2016).

[33] F. Wächtler and L. Santos, Phys. Rev. A **94**, 043618 (2016).

[34] I. Ferrier-Barbut, M. Schmitt, M. Wenzel, H. Kadau, and T. Pfau, J. Phys. B: At. Mol. Opt. Phys. **49**, 214004 (2016).

[35] C. R. Cabrera, L. Tanzi, J. Sanz, B. Naylor, P. Thomas, P. Cheiney, and L. Tarruell, Science **359**, 301 (2018).

[36] G. Semeghini, G. Ferioli, L. Masi, C. Mazzinghi, L. Wolswijk, F. Minardi, M. Modugno, G. Modugno, M. Inguscio, and M. Fattori, Phys. Rev. Lett. **120**, 235301 (2018).

[37] D. Baillie and P. B. Blakie, Phys. Rev. Lett. **121**, 195301 (2018).

[38] S. M. Roccuzzo and F. Ancilotto, Phys. Rev. A **99**, 041601 (2019).

[39] P. Naidon and D. S. Petrov, Phys. Rev. Lett. **126**, 115301 (2021).

[40] O. Penrose and L. Onsager, Phys. Rev. **104**, 576 (1956).

[41] A. J. Leggett, *Quantum Liquids* (Oxford University Press, 2006).

[42] H. T. C. Stoof, B. G. Koss, and D. B. M. Dickerscheid, *Ultracold Quantum Fields* (Springer, 2009).

[43] N. N. Bogoliubov, J. Phys. (USSR) **11**, 23 (1947).

[44] A. Griffin, T. Nikuni, and E. Zaremba, *Bose-Condensed Gases at Finite Temperatures* (Cambridge University Press, 2009).

[45] N. N. Bogoliubov, *Lectures on Quantum Statistics: Quasi-Averages*, Vol. 2 (Gordon and Breach, 1970).

[46] N. M. Hugenholtz and D. Pines, Phys. Rev. **116**, 489 (1959).

[47] A. L. Fetter, Ann. Phys. (N. Y.) **70**, 67 (1972).

[48] E. P. Gross, Nuovo Cimento **20**, 454 (1961).

[49] L. P. Pitaevskii, Zh. Eksp. Teor. Fiz. **40**, 646 (1961).

[50] L. P. Pitaevskii, Sov. Phys. JETP **13**, 451 (1961).

[51] P. G. de Gennes, *Superconductivity of Metals and Alloys* (Addison-Wesley, 1989).

[52] A. Griffin, Phys. Rev. B **53**, 9341 (1996).

[53] S. Giorgini, L. P. Pitaevskii, and S. Stringari, J. Low Temp. Phys **109**, 309 (1997).

[54] T. Lahaye, C. Menotti, L. Santos, M. Lewenstein, and T. Pfau, Rep. Prog. Phys. **72**, 126401 (2009).

[55] K. Góral, K. Rzazewski, and T. Pfau, Phys. Rev. A **61**, 051601 (2000).

[56] A. L. Fetter and J. D. Walecka, *Quantum Theory of Many-Particle Systems* (Dover, 2003).

[57] A. Boudjemâa, J. Phys. A: Math. Theor. **49**, 285005 (2016).

[58] H. Saito, J. Phys. Soc. Jpn. **53**, 053001 (2016).

[59] A. Macia, J. Sánchez-Baena, J. Boronat, and F. Mazzanti, Phys. Rev. Lett. **117**, 205301 (2016).

[60] A. Bulgac, Phys. Rev. Lett. **89**, 050402 (2002).

[61] D. S. Petrov and G. E. Astrakharchik, Phys. Rev. Lett. **117**, 100401 (2016).

[62] D. S. Petrov and G. V. Shlyapnikov, Phys. Rev. A **64**, 012706 (2001).

[63] M. Olshanii, Phys. Rev. Lett. **81**, 938 (1998).

[64] G. E. Astrakharchik and B. A. Malomed, Phys. Rev. A **98**, 013631 (2018).

[65] E. H. Lieb and W. Liniger, Phys. Rev. **130**, 1605 (1963).

[66] G. B. Hess and W. M. Fairbank, Phys. Rev. Lett. **19**, 216 (1967).

[67] P. J. Bendt, Phys. Rev. **127**, 1441 (1962).

[68] J. D. Reppy and D. Depatie, Phys. Rev. Lett. **12**, 187 (1964).

[69] L. Landau, J. Phys. USSR **5**, 71 (1941).

[70] L. Tisza, Nature **141**, 913 (1938).

[71] M. Holzmann and G. Baym, Phys. Rev. Lett. **90**, 040402 (2003).

[72] P. Nozierès and D. Pines, *The Theory of Quantum Liquids: Superfluid Bose Liquids*, Vol. 2 (CRC Press, 1990).

[73] D. A. Butts and D. S. Rokhsar, Nature **397**, 327 (1999).

[74] G. M. Kavoulakis, B. Mottelson, and C. J. Pethick, Phys. Rev. A **62**, 063605 (2000).

[75] E. Lundh, Phys. Rev. A **65**, 043604 (2002).

[76] G. M. Kavoulakis and G. Baym, New J. Phys. **5**, 51 (2003).

[77] V. K. Tkachenko, Zh. Eksp. Teor. Fiz. **49**, 1875 (1965).

[78] J. R. Abo-Shaeer, C. Raman, M. Vogelsand, and W. Ketterle, Science **292**, 476 (2001).

[79] C. Ryu, M. F. Andersen, P. Cladé, V. Natarajan, K. Helmerson, and W. D. Phillips, Phys. Rev. Lett. **99**, 260401 (2007).

[80] A. Ramanathan, K. C. Wright, S. R. Muniz, M. Zelan, W. T. Hill, C. J. Lobb, K. Helmerson, W. D. Phillips, and G. K. Campbell, Phys. Rev. Lett. **106**, 130401 (2011).

[81] S. Komineas, N. R. Cooper, and N. Papanicolaou, Phys. Rev. A **72**, 053624 (2005).

[82] M. Boninsegni and N. V. Prokof'ev, Rev. Mod. Phys. **84**, 759 (2012).

[83] A. J. Leggett, Journal of Statistical Physics **93**, 927 (1998).

[84] L. Santos, G. V. Shlyapnikov, and M. Lewenstein, Phys. Rev. Lett. **90**, 250403 (2003).

[85] D. H. J. O'Dell, S. Giovanazzi, and G. Kurizki, Phys. Rev. Lett. **90**, 110402 (2003).

[86] L. Chomaz, R. M. W. van Bijnen, D. Petter, G. Faraoni, S. Baier, J. H. Becher, M. J. Mark, F. Wächtler, L. Santos, and F. Ferlaino, Nat. Phys. **14**, 442 (2018).

[87] H. Kadau, M. Schmitt, M. Wenzel, C. Wink, T. Maier, I. Ferrier-Barbut, and T. Pfau, Nature **530**, 194 (2016).

[88] G. Natale, R. M. W. van Bijnen, A. Patscheider, D. Petter, M. J. Mark, L. Chomaz, and F. Ferlaino, Phys. Rev. Lett. **123**, 050402 (2019).

[89] J. L. Bohn, R. M. Wilsom, and S. Ronen, Laser Phys. **19**, 547 (2009).

[90] A. Gallemí, S. M. Roccuzzo, S. Stringari, and A. Recati, Phys. Rev. A **102**, 023322 (2020).

[91] Y.-C. Zhang, F. Maucher, and T. Pohl, Phys. Rev. Lett. **123**, 015301 (2019).

[92] F. Ancilotto, M. Barranco, M. Pi, and L. Reatto, Phys. Rev. A **103**, 033314 (2021).

[93] S. M. Roccuzzo, S. Stringari, and A. Recati, Phys. Rev. Research **4**, 013086 (2022).

[94] F. Böttcher, M. Wenzel, J.-N. Schmidt, M. Guo, T. Langen, I. Ferrier-Barbut, T. Pfau, R. Bombín, J. Sánchez-Baena, J. Boronat, and F. Mazzanti, Phys. Rev. Research **1**, 033088 (2019).

[95] D. Petter, G. Natale, R. M. W. van Bijnen, A. Patscheider, M. J. Mark, L. Chomaz, and F. Ferlaino, Phys. Rev. Lett. **122**, 183401 (2019).

[96] M. Ota and G. E. Astrakharchik, SciPost Phys. **9**, 020 (2020).

[97] H. Hu and X.-J. Liu, Phys. Rev. Lett. **125**, 195302 (2020).

[98] H. Hu, J. Wang, and X.-J. Liu, Phys. Rev. A **102**, 043301 (2020).

LUND
UNIVERSITY

Faculty of Engineering
Department of Physics
Division of Mathematical Physics